

T.R.
GEBZE TECHNICAL UNIVERSITY
GRADUATE SCHOOL OF NATURAL AND APPLIED SCIENCES

SIDE CHAIN LIQUID CRYSTALLINE POLYMERS FOR
ORGANIC FIELD EFFECT TRANSISTORS

ÇİĞDEM ÇAKIRLAR
A THESIS SUBMITTED FOR THE DEGREE OF
MASTER OF SCIENCE
DEPARTMENT OF PHYSICS

GEBZE
2015

T.R.
GEBZE TECHNICAL UNIVERSITY
GRADUATE SCHOOL OF NATURAL AND APPLIED SCIENCES

**SIDE CHAIN LIQUID CRYSTALLINE
POLYMERS FOR ORGANIC FIELD
EFFECT TRANSISTORS**

ÇİĞDEM ÇAKIRLAR
**A THESIS SUBMITTED FOR THE DEGREE OF
MASTER OF SCIENCE
DEPARTMENT OF PHYSICS**

THESIS SUPERVISOR
PROF. DR. SAİT EREN SAN

GEBZE
2015

T.C.
GEBZE TEKNİK ÜNİVERSİTESİ
FEN BİLİMLERİ ENSTİTÜSÜ

ORGANİK ALAN ETKİLİ
TRANSİSTÖRLER İÇİN YAN GRUP SIVI
KRİSTAL POLİMERLER

ÇİĞDEM ÇAKIRLAR
YÜKSEK LİSANS TEZİ
FİZİK ANABİLİM DALI

DANIŞMANI
PROF. DR. SAİT EREN SAN

GEBZE
2015

GEBZE TEKNİK ÜNİVERSİTESİ	YÜKSEK LİSANS JÜRİ ONAY FORMU
----------------------------------	--------------------------------------

GTÜ Fen Bilimleri Enstitüsü Yönetim Kurulu'nun 29/12/2014 tarih ve 2014/73 sayılı kararıyla oluşturulan jüri tarafından 19/01/2015 tarihinde tez savunma sınavı yapılan Çiğdem ÇAKIRLAR' ın tez çalışması Fizik Anabilim Dalında YÜKSEK LİSANS tezi olarak kabul edilmiştir.

JÜRİ

ÜYE

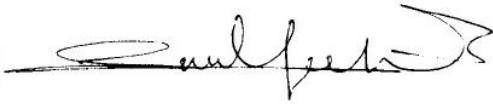
(TEZ DANIŞMANI)

: Prof. Dr. Sait Eren SAN




ÜYE

: Prof. Dr. Yusuf YERLİ



ÜYE

: Doç. Dr. Savaş BERBER



ONAY

Gebze Teknik Üniversitesi Fen Bilimleri Enstitüsü Yönetim Kurulu'nun
...../...../..... tarih ve/..... sayılı kararı.

İMZA/MÜHÜR

SUMMARY

Transistors are at the heart of electronic devices with their switching, amplification and sensor properties. Inexpensive, lightweight and eco-friendly organic electronic devices, especially layer by layer processed Organic Field Effect Transistors (OFET) gives lots of opportunity when compared with well-known inorganic based devices. Poly (methyl-methacrylate) (PMMA) is quite common material for OFET production, with its easy processing to various surfaces, very low manufacturing cost and relatively high dielectric constant. In last decade, researches and investigations indicate that liquid crystalline derivative of PMMA is very attractive material for OFET applications.

In this study, electrical analysis was performed to thin films, which was produced from different molecular weight of PMMA. Due to their film morphology and dielectric properties, best suitable material is chosen. Electrical analysis of homo-polymer poly (Chol-n-MMA) and co-polymer poly (Chol-n-MMA-co-MMA) with aliphatic spacer length $n=3, 7, 10$ was carried out with HP 4194 A between 100 Hz and 15 MHz at room temperature. OFETs are produced according to dielectric analysis. These produced OFETs are characterized by using Keitley 4200 SCS. Transfer and output characteristics are investigated. Experimental results show that this material is very promising for future OFET applications, particularly electronic papers and new age textile products.

Key Words: Organic Field Effect Transistor, Gate Dielectric, Side Chain Liquid Crystal, Polymethy metacrylate(PMMA), Conduction Mechanism.

ÖZET

Transistörler anahtarlama, yükseltici ve sensör özellikleri ile elektronik cihazların kalbinde yer almaktadırlar. Ucuz, hafif ve çevreci organik elektronik cihazlar, özellikle katman katman üretilen organik alan etkili transistörler (Organic Field Effect Transistors- OFET) var olan inorganik tabanlı transistor teknolojisine alternatif çözümler sunmaktadır.

Ortam koşullarındaki kararlılığı, farklı yüzeylere uygulanabilirliği, işlem maliyetlerinin düşük olması ve nispeten yüksek dielektrik sabiti değerine sahip olması nedeniyle PMMA, OFET üretimi için yaygın olarak tercih edilen bir dielektrik malzemedir. Son on yılda yapılan çalışmalar ve incelemeler ışığında PMMA'nın sıvı kristal türevlerinin OFET uygulamaları için ilgi çekici özellikleri olduğu anlaşılmıştır.

Bu çalışmada farklı molekül ağırlıklarındaki PMMA'dan üretilen ince filmlerinin elektriksel özellikleri incelenmiş; yalıtkanlık özellikleri yanı sıra film morfolojileri de göz önüne alınarak uygun molekül ağırlığında malzeme seçilmiştir. Seçilen polimerden sentezlenen poli (Chol-n-MMA) homo-polimerinin ve poli (Chol-n-MMA-co-MMA) kopolimerinin (alifatik boşluk uzunluğu $n = 3, 7, 10$ olan) elektriksel analizi HP 4194 A model empedans analizörü kullanılarak oda sıcaklığında yapılmıştır. Analiz edilen bu malzemelerden OFET üretilmiş ve Keitley 4200 SCS model yarı iletken karakterizasyon cihazı ile transfer karakteristikleri ve output karakteristikleri incelenmiştir.

Deney sonuçları göstermiştir ki, bu malzemenin elektriksel özellikleri OFET uygulamaları, özellikle yeni nesil elektronik kağıtlar ve tekstil ürünlerinin üretimi için gelecek vadetmektedir.

Anahtar Kelimeler: Organik Alan Etkili Transistörler, Kapı Yalıtkanı, Yan Zincir Sıvı Kristaller, Polymethy metacrylate(PMMA), İletkenlik Mekanizması.

ACKNOWLEDGEMENTS

Firstly I would like to thank to my supervisor Prof. Dr. Sait Eren San for all of guidance throughout this project.

Words fail when I wish to describe my appreciation to Assoc. Prof. Dr. Mustafa Okutan, whose personality was actually an inspiration for this work.

Also thanks to Prof. Dr Yusuf Yerli not only for their help on device design and scientific discussion but also encouragements during my working period.

I am very grateful to Assoc. Prof. Dr. Faruk Yılmaz and my colleagues Dr. Erdinç Dođancı and Sümeyra Bayır for synthesizing dielectric materials and their guidance.

I owe Assoc. Prof. Dr. Paweł Perkowski a debt of gratitude for his kind interest and comments for technical graphs.

Thank you to my colleagues, past and present, in the GIT Organic Electronic Laboratory, mostly Dr. Eşe Akpınar and Muhammad Yasin for their friendship and help. I am appreciating to Gökhan Bayram for all his guidance and help for the generations of device schematics.

Finally thanks to my parents for their financial support and great love, all the time of my life.

In this study all examined dielectric polymers have been synthesized within TUBİTAK 1001 Project, with Project Number:112T846.

This thesis is supported by National Scholarship Program for Graduate Student TUBİTAK (2211) in MSc thesis.

TABLE of CONTENTS

	<u>Page</u>
SUMMARY	v
ÖZET	vi
ACKNOWLEDGEMENTS	vii
TABLE of CONTENTS	viii
LIST of ABBREVIATIONS and ACRONYMS	x
LIST of FIGURES	xiii
LIST of TABLES	xvi
1. INTRODUCTION	1
1.1. Brief Explanation of OFET	2
2. DIELECTRIC THEORY and OFET	11
2.1. Dielectric Theory	11
2.1.1. Dielectrics	11
2.1.2. Dielectric Parameters	12
2.1.3. Cole-Cole Plots	16
2.2 Organic Field Effect Transistor (OFET)	17
2.2.1 Basic Device Structure and Physics	17
2.2.2. Charge Transport	19
2.2.3. Current Voltage Characteristics	22
3. MATERIALS and EXPERIMENTAL PART	25
3.1 Thin Film Capacitor Fabrication	25
3.2. Spectroscopic Analysis of Polymeric Thin Films	29
3.3 OFET Fabrication	29
3.3.1 Organic Semiconductor	31
3.3.2. Gate Dielectric	32
3.3.3. Metal Electrode	32
4. RESULTS	33
4.1. Dielectric Results	33
4.2 OFET Results	44
5. CONCLUSION	47

REFERENCES

48

BIOGRAPHY

52

LIST of ABBREVIATIONS and ACRONYMS

<u>Abbreviations</u>	<u>Explanations</u>
<u>and Acronyms</u>	
Δ	: Delta
\square	: Absorption Coefficient
C	: Capacity
<i>E</i>	: Electrical Field Vector
ϵ_0	: Dielectric Permittivity of Vacuum
ϵ'	: Real Part of Complex Dielectric Constant
ϵ''	: Imaginary Part of Complex Dielectric Constant
ϵ_r	: Relative Permittivity
ϵ_s	: Dielectric constant at lowest frequency
ϵ_∞	: Dielectric constant at highest frequency
ϵ	: Dielectric Constant
$\epsilon'(\omega)$: Frequency dependent real part of dielectric constant
$\epsilon''(\omega)$: Frequency dependent imaginary part of dielectric constant
I_D	: Drain Current
I_G	: Gate Current
Q	: Electrical Charge
L	: Channel Length of OFET
μ	: Mobility
μ_{FET}	: Field Effect Mobility
μ_p	: Hole mobility
μ_n	: Electron mobility
μm	: Micrometer
M	: Molecular Weight
n	: Molecular Orientation Vector Of Cholesteric Liquid Crystal
n	: Aliphatic spacer length of side chain liquid crystal
N_A	: Avogadro Number
P	: Polarization Vector
ρ	: Density
s	: S parameter

τ_0	:	Relaxation Time
ν	:	Frequency
V	:	Potential
V_{GS}	:	Gate-Source Voltage
V_{DS}	:	Source-Drain Voltage
V_{th}	:	Threshold Voltage
$V_{th,p}$:	Threshold Voltage of P Type Material
$V_{th,n}$:	Threshold Voltage of N Type Material
AC	:	Alternating Current
Ag	:	Silver
Al	:	Aluminum
AMOLED	:	Active Matrix Organic Light Emitting Diode
Au	:	Gold
CBH	:	Correlated barrier hopping
CYEPL	:	Cyanoethylpullulan
DC	:	Direct Current
FET	:	Field Effect Transistor
Ge	:	Germanium
GIT	:	Gebze Institute of Technology
HP	:	Hewlett Packard
HOMO	:	Highest Occupied Molecular Orbital
Hz	:	Hertz
ITO	:	Indium Tin Oxide
LC	:	Liquid crystal
LUMO	:	Lowest Occupied Molecular Orbital
MEH-PPV	:	Poly(2-methoxy-5-(2-ethylhexyloxy)-1,4-phenylenevinylene)
MHz	:	Megahertz
mm	:	Millimeter
OLED	:	Organic Light Emitting Diode
OPV	:	Organic Photo Voltaic
OTFT	:	Organic Thin Film Transistor
P3HT	:	Poly(3-hexylthiophene)
PCBM	:	Phenyl-C61-butyric acid methyl ester

PMMA	:	Poly (methyl methacrylate)
Poly(ChM MA-n)	:	Poly (Cholesteryl n-methacryloxybutyrate)
Poly (ChMMA- n-co- MMA)	:	Poly (Cholesteryl n-methacryloxybutyrate-co-methyl methacrylate)
PS	:	Polystyrene
PVA	:	Polyvinyl alcohol
PVC	:	Polyvinyl chloride
RC	:	Resistance-Capacitance
RFID	:	Radio Frequency Identity
rpm	:	Rotation Per Minute
SCLC	:	Side Chain Liquid Crystal
SLPL	:	Super Linear Position Law
Si	:	Silicium
SiO ₂	:	Silicon Dioxide
THF	:	Tetrahydrofuran
QMT	:	Quantum Mechanical Tunneling

LIST of FIGURES

<u>Figure No:</u>	<u>Page</u>
1.1 : a) and b) are examples of produced flexible OFETs.	1
1.2 : OTFT screen produced by Sony Inc.	2
1.3 : Different structures a) Top contact / bottom gate b) Bottom contact / bottom gate c) Bottom contact / top gate d) Top contact / top gate.	3
1.4 : Example of Top gate/bottom contact OFET structure.	4
1.5 : Charge carrier transfer mechanism of a top contact/bottom gate OFET with a) n-type semiconductor b) p- type semionductor.	5
1.6 : Organic semiconductor polymers' molecular structure a) p3ht b) PCBM.	6
1.7 : Molecular structure of PMMA.	7
1.8 : Schematic illustration of a) crystal b) liquid crystal c) liquid phase of matter.	8
1.9 : Classification of liquid crystals.	9
1.10: Schematic illustration of Nematic a), Cholesteric b), Smectic c) phase of liquid crystals.	10
1.11: Schematic illustration of OFET with SCLCP dielectric layer	10
2.1 : Parallel plate capacitor.	11
2.2 : Dielectric material without orientation between two parallel plates b) Orientational polarization due to applied electric field.	13
2.3 : Representation of frequency dependent relaxation mechanisms in polar dielectric materials.	14
2.4 : The schematic illustration of OFET band structure with a) P-type organic semiconductor b) N-type organic semiconductor.	18
2.5 : Demonstration of channel length and channel width of OFET	19
2.6 : Equivalent circuit model of an OFET.	20
2.7 : Schematic and b) graphical illustration of Operation modes of OFET.	21
2.8 : Typical transfer characteristics of a polymer OFET	23
2.9 : Output characteristics of the same polymer OFET.	23

2.10:	Threshold voltage determination of an OFET.	24
3.1 :	Thermal oven.	26
3.2 :	a) Schematic illustration spin coating and annealing process b) spin coater.	27
3.3 :	Veeco Dektak 8 profilometer.	27
3.4 :	Leybold Thermal Evaporator.	28
3.5 :	Thin film capacitor.	28
3.6 :	HP 4194 A Gain/Impedance Analyzer.	29
3.7 :	Preparation of organic semiconducting polymer (P3HT) solution	30
3.8 :	Prepared silver source- drain contacts.	31
4.1 :	Frequency dependent real part of dielectric constant of PMMA homo-polymers with different molecular wight.	33
4.2 :	Equivalent circuits of thin film capacitors of samples.	36
4.3 :	Frequency dependent real part of dielectric constant of poly(chol-3-MMA-co-MMA), with SCLC ratio 10%, 5%, 3%, 2%, 1% and 0.5%.	38
4.4 :	Frequency dependent imaginary part of dielectric constant of poly(chol-3-MMA-co-MMA), with SCLC ratio 10%, 5%, 3%, 2%, 1% and 0.5%.	39
4.5 :	Specific conductivity plot of poly (chol-3-MMA-co-MMA), with SCLC ratio 10%, 5%, 3%, 2%, 1% and 0.5%.	39
4.6 :	Plot of $\ln(\epsilon_{(AC)})$ versus $\ln(\epsilon)$ of Poly (chol-3-MMA-co-MMA) with SLCL ratio 0.5%	40
4.7 :	Plot of $\ln(\epsilon_{(AC)})$ versus $\ln(\epsilon)$ of Poly (chol-3-MMA-co-MMA) with SLCL ratio 1%.	41
4.8 :	Plot of $\ln(\epsilon_{(AC)})$ versus $\ln(\epsilon)$ of Poly (chol-3-MMA-co-MMA) with SLCL ratio 2%.	41
4.9 :	Plot of $\ln(\epsilon_{(AC)})$ versus $\ln(\epsilon)$ of Poly (chol-3-MMA-co-MMA) with SLCL ratio 3%.	42
4.10:	Plot of $\ln(\epsilon_{(AC)})$ versus $\ln(\epsilon)$ of Poly (chol-3-MMA-co-MMA) with SLCL ratio 5%.	42
4.11:	Plot of $\ln(\epsilon_{(AC)})$ versus $\ln(\epsilon)$ of Poly (chol-3-MMA-co-MMA) with SLCL ratio 10%.	43
4.12:	Cole-Cole plots of plot of Poly (chol-3-MMA-co-MMA) with SLCL.	44

4.13: Output characteristic of prepared OFET.	45
4.14: Transfer characteristic of fabricated OFET.	46

LIST of TABLES

<u>Table No:</u>	<u>Page</u>
1.1: Dielectric constants of some organic materials.	8
3.1: Investigated dielectric materials.	25
3.2: Solution ratios of PMMA samples.	26
4.1: Absorption coefficient α , relaxation time (τ_0), dielectric parameters (ϵ_s , ϵ_∞ , ϵ''_{max} , and $\Delta\epsilon$) and critical frequencies (f_c) of Poly(Chol-n-MMA) and poly(Chol-n-MMA-co-MMA) (n= 3, 7, and 10).	35
4.2: Definition of conduction mechanism according to s parameter.	36
4.3: Absorption coefficient α , relaxation time (τ_0), dielectric parameters (ϵ_s , ϵ_∞ , ϵ''_{max} , and $\Delta\epsilon$) and critical frequencies (f_c) of poly(Chol-3-MMA-co-MMA) with SCLC ratio 10%, 5%, 3%, 2%, 1% and 0.5%.	37

1. INTRODUCTION

In recent years, investigation of organic microelectronic devices has attracted attention of the researchers due to their low cost, lightweight, ease of processing at low temperatures, flexibility, large area capability and various promising applications. Organic Solar Cells, Organic Thin Film Transistors, Organic Light Emitting Diodes and Transistors are few prominent examples of these devices [1], [2], [3]. Their applications include flexible displays, large area force sensing, ultrasonic mapping, and active matrix imaging. Also it gives opportunity to integrate circuits to textile products, bioelectronics skins and muscles [4], [5]. Some of these prototype devices are given in Figure 1.1 and Figure 1.2 [6], [7].

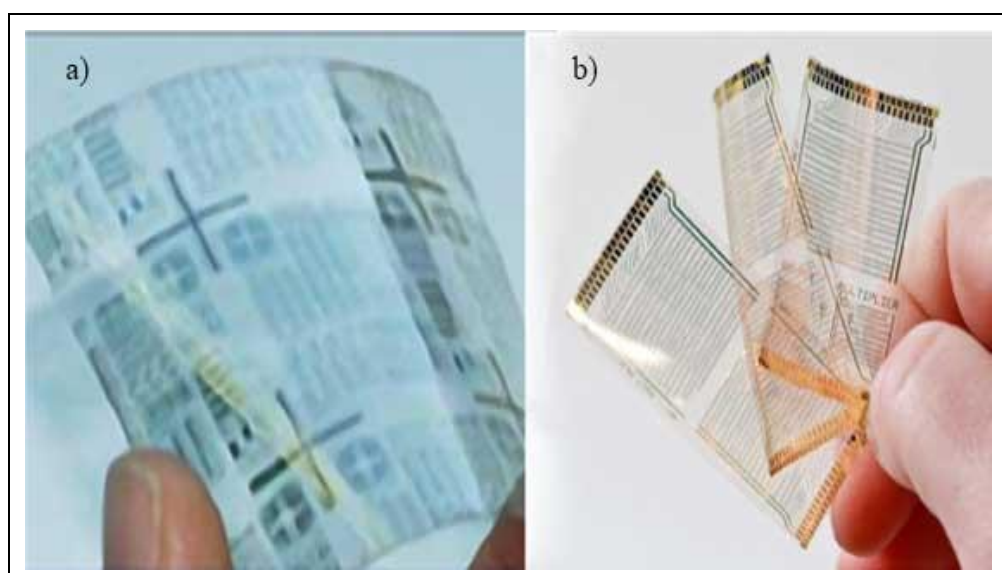


Figure 1.1: a) and b) are examples of produced flexible OFETs.

Some of these devices are commercially available and took their place in the markets [8]. But still some handicaps exist, like low mobility of organic semiconductors, low durability on environmental conditions [9]. Organic field effect transistors (OFET) are one of faster device of them.



Figure 1.2 OTFT screen produced by Sony Inc.

OFETs are field effect transistor, which includes organic semiconductor layer as an active channel. OFETs are three terminal devices with two ohmic contacts; source drain and third contact, gate [10]. Basic structures of OFET consist of two layers. First one is organic semiconductor and second dielectric layer. The dielectric layer has crucial importance since it is the location where charge transport in the channel occurs. The gate dielectric layer controls the charge carriers induced in the channel by the gate voltage [11]. Due to this reason, gate dielectric has quite important role in device fabrication. Interface interaction between organic semiconductor and gate dielectric is pretty essential. To overcome all the possible difficulties, choosing suitable and compatible material is necessary [12].

It is known that liquid crystals have peculiar behavior with different physical conditions such as temperature and electrical field. That is the reason of preference of LCP as dielectric layer in literature [13] Smectic phase is one of the liquid crystalline phase, which is very promising with its electro and thermo optical applications for organic electronics.

1.1. Brief Explanation of OFET

OFETs are fabricated with various structures, basically four types are very well known. Two of them is named as bottom gate and others top gate. Contact location is different with every structure. This will effect; on/off ratio, interface properties of

semiconductor and gate dielectric, leakage current from gate contact and also mobility of charge carriers.

Structures must be chosen according to the properties of materials for desired OFET. All of these popular structures are given in Figure 1.3.

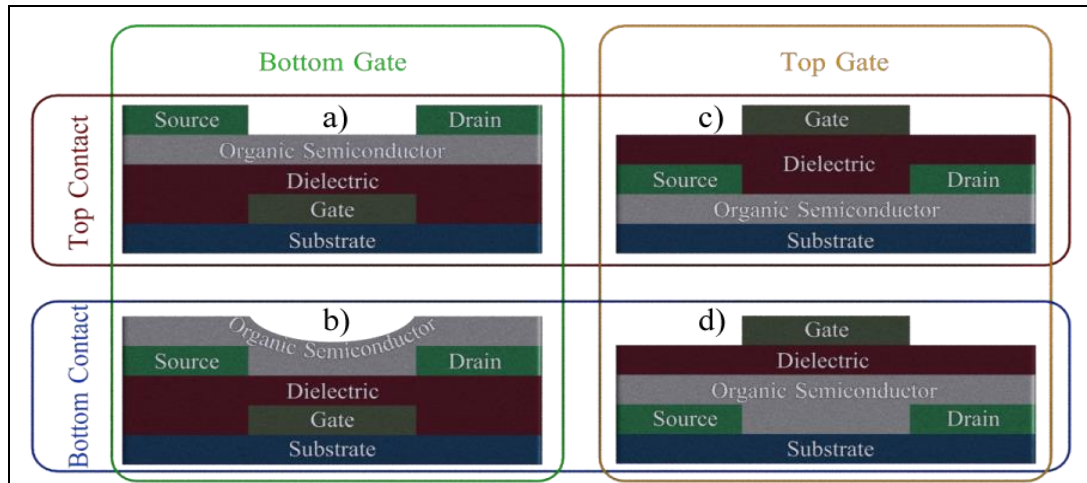


Figure 1.3: Different structures a) Top contact / bottom gate b) Bottom contact / bottom gate c) Bottom contact / top gate d) Top contact / top gate.

The best-preferred structure is bottom gate / top contact structure, is given in Figure 1.3 OFETs produced by bottom gate structure give possibility to get better film morphology and reduce surface interactions. Top gate/bottom contact is another structure design, which is suitable to install the organic films on flexible substrates [6]. So that, it gives chance to get smart clothes, artificial skin, electronic papers and RFID tags applications [14].

- Working Principle of OFETs

OFET is three terminal device, source and drain electrodes are connected to the semiconductor layer, whereas the gate electrode is electrically insulated from the semiconductor by the gate dielectric layer. Basically, field effect transistors operate as a capacitor whose one plate is highly conductive metal and other is semiconductor layer, separated by one or more dielectric layer. When some bias induced to metal electrode, that cause segregation of charges in dielectric material, thereby an accumulation of charges occur in semiconductor part [10].

Thin region between source and drain is called as channel. FETs are working with the variation principle of current, passing through between two ohmic contact (source and drain) with bias of insulator covered, third contact (gate) [7]. This current that passing through channel depends on both gate and drain voltage. Various operation regimes can be obtained with different applied bias.

Organic semiconductor can be both p-type and n-type. Gate bias is given according to type of organic semiconductors. Gate voltage supply the dissociation of positive and negative carriers on gate dielectric.

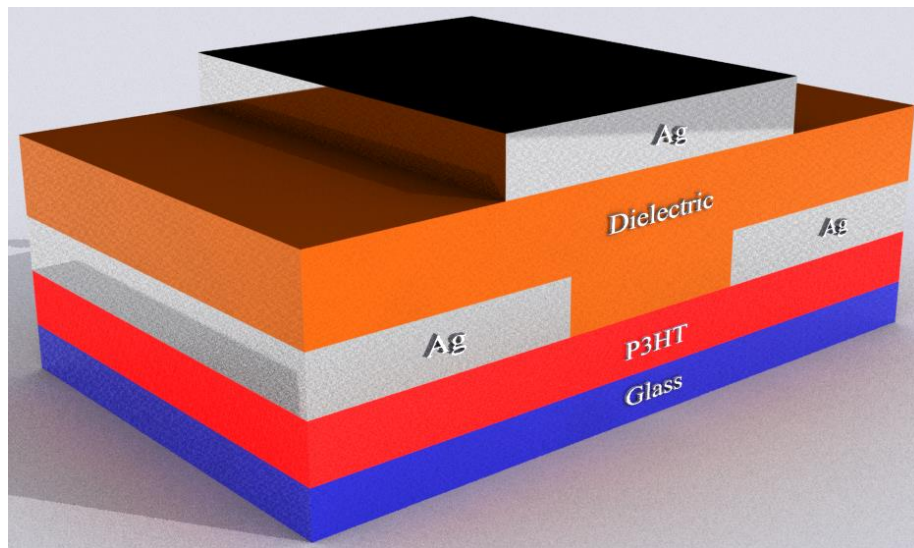


Figure 1.4: Example of Top gate/bottom contact OFET structure.

In this thesis, organic field effect transistors are discussed which is operating in unipolar p-type accumulation mode given in Figure 1.4. In other words positive charge carriers are the cause of current in the channel, which is illustrated in Figure 1.5.

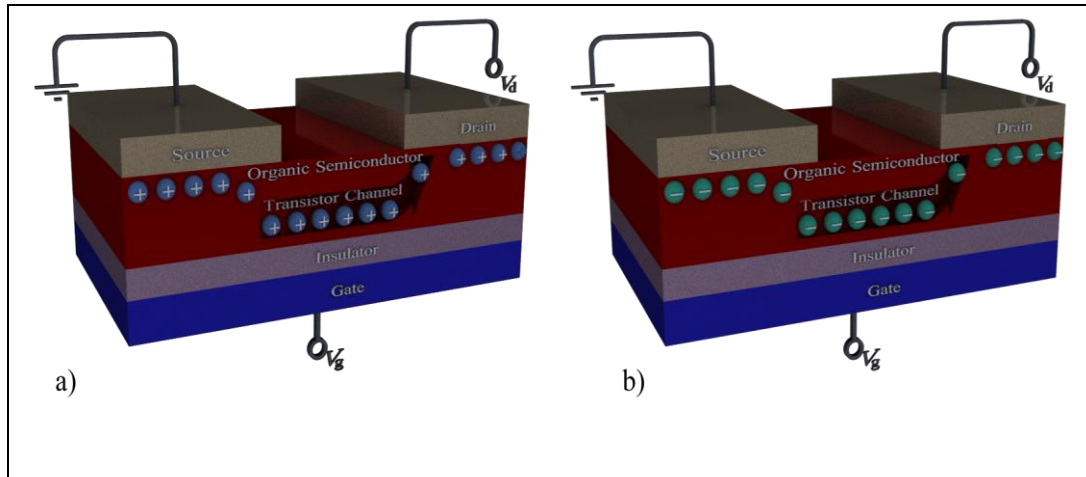


Figure 1.5: Charge carrier transfer mechanism of a top contact/bottom gate OFET with a) p-type semiconductor b) n- type semiconductor.

- Organic Semiconductor Polymers

Until 1970's all the carbon based polymers are known as insulator. They were used for insulation of electrical systems. So that, using polymers as conductor is not reasonable. However, there are at least four major types of semiconducting polymers that have been developed up to now. These are conjugated conducting polymers, charge transfer polymers, ionically conducting polymers and conductively filled polymers [15].

In this study, one of the conjugated conducting polymers is used as organic semiconductor material. These polymers have too many unusual optoelectronic properties, which allow conjugated polymers to be used for a huge number of applications, including protecting metals from corrosion [16], sensing devices, artificial actuators [17], organic transistors [7], non-linear optical devices and light-emitting displays [18]. However conjugated polymer still suffer with insolubility, infusibility, brittleness and even instability in air [19]. Conjugate polymers are widely used in organic electronic application, that is why consideration of conduction mechanism of them is very vital. Some of them is demonstrated in Figure 1.6 [20].

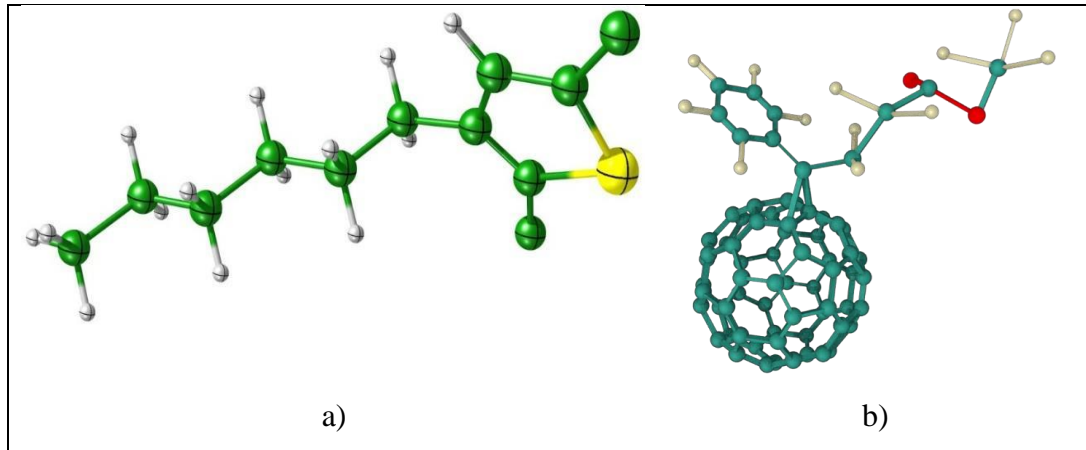


Figure 1.6: Organic semiconductor polymers' molecular structure a) P3HT b) PCBM.

- Conduction Mechanism In Conjugate Polymers

Conjugated polymers are macromolecules, which has sequential single and double bonds. In 1977, Alan J. Heeger Alan G. MacDiarmid and Hideki Shirakawa were observed that Polyacetylene could show higher degree of conductivity when compared with other insulators. They were rewarded with Nobel chemistry prize with this study in 2000 [21].

All the conjugated polymers have delocalized π electrons. Unlike the σ bond, which is localized to two adjacent carbon atoms, the π electrons are shared and delocalized among a molecule, making losing such an electron is not energetically significant [22].

These π bonds are weaker than σ bonds, and can be accepted as the reason of conduction in semiconducting polymers. Excitation energy of conjugated π electrons are generally at the range of visible range. To attain conduction from this polymers some dope process is required like inorganic semiconductors [21], [23].

Poly(3-hexylthiophene) (P3HT), Poly(2-methoxy-5-(2-ethylhexyloxy)-1,4-phenylenevinylene) (MEH-PPV) are just of two widely used conjugated polymers. These conjugated polymers can be dissolved in solvents like toluene, tetrahydrofuran, chloroform, and dichlorobenzene. That is a great convenience for making polymer films with doctor blading, spin coating, inkjet printing, dip coating, and spray coating techniques [24], [25], [26]. As a result producing low cost devices can be possible.

- Organic Dielectric Materials- PMMA

In recent history, conventional silicon dioxide (SiO_2) has preponderated electronics as the preferred gate dielectric material. Nevertheless, it does not provide many of the performance requirements with its relatively low dielectric constant ($\epsilon' \approx 3.9$), expensive and challenging production processes [27], [28].

Organic dielectric materials are solution processable materials. Whereby, they are promising for flexible electronics and optoelectronics.

To decrease the gate voltage of a field effect transistor, gate dielectric must be well chosen. Decreasing of energy consumption can be provided with reducing gate voltage. Not only high dielectric constant is required but also interfaces interaction and easy processing is both important. Dielectric constants of some organic dielectric materials is given in Table 1.1 [28].

PMMA is very popular dielectric materials for OFETs whose dielectric constant (ϵ') is around 3.5 [28]. It can be soluble in water, toluene, tetrahydrofurane (THF) and ethyl acetate, which give a great chance to diminish expense of manufacturing process. Although it has low dielectric constant, it gives opportunity to obtain better new sensitized polymers with various polymerization techniques. Its molecular structure is given in Figure 1.7.

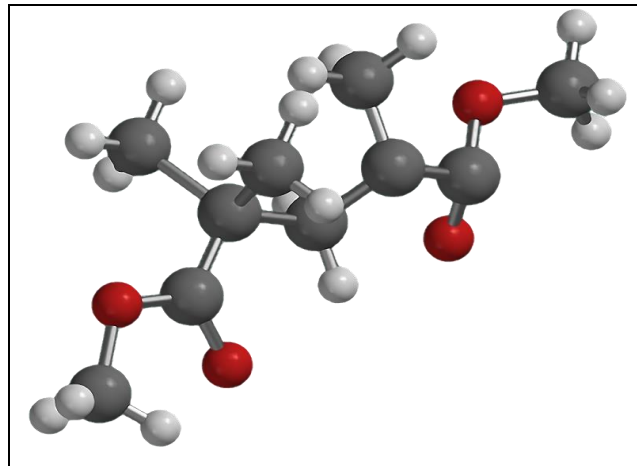


Figure 1.7: Molecular structure of PMMA.

Table 1.1: Dielectric constants of some organic materials.

Organic Dielectric Materials	Dielectric Constants
PVA	7.8
PS	2.6
PVC	4.6
CYEPL	18.5
PMMA	3.5

- Liquid Crystals

Liquid crystals are intermediate state of matter, in between the liquid and the crystal. It must have some characteristic features of a liquid (e. g. fluidity, inability to support shear, formation and coalescence of droplets) also some crystalline properties (anisotropy in optical, electrical, and magnetic properties, periodic arrangement of molecules in one spatial direction, etc.).

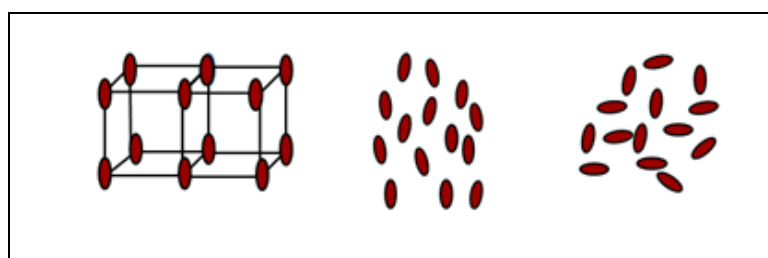


Figure 1.8: Schematic illustration of a) crystal b) liquid crystal c) liquid phase of matter.

Phases of matter are demonstrated in Figure 1.8. At certain condition (such as temperature) liquid crystals are at solid phase, applying melting temperature they will become liquid crystal. They will have long-range order orientation. If the temperature will continuously increasing liquid crystal will change their phase as liquid. Its appearance will be blurry and viscous. This material will show totally isotropic properties. Different types of liquid crystals are given in Table 1.2.

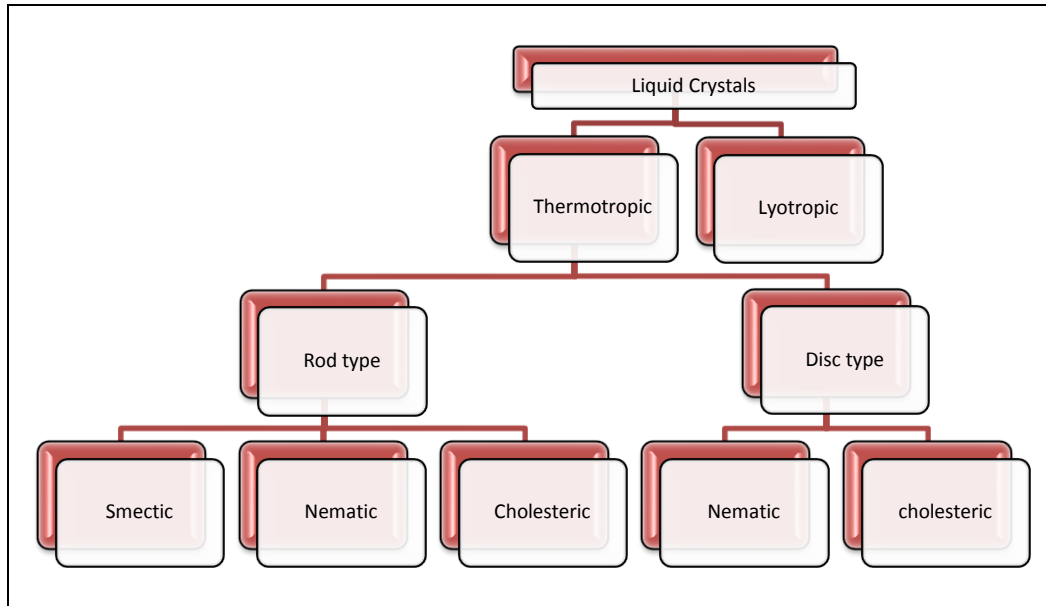


Figure 1.9: Classification of liquid crystals.

In this study, rod type liquid crystals are investigated and their basic properties are given below, also their schematic illustration is also given in Figure 1.10.

Nematic liquid crystals: This type is very similar to liquids; molecules can be freely positioned but oriented parallel to each other. It is clearly seen three-dimensional scheme of nematic liquid crystals at in Figure 1.9 a). Molecular orientation is generally described with vector \mathbf{n} in else where.

Cholesteric liquid crystals: This type of liquid crystals is generally observed with derivation of cholesterol. Cholesteric phase is consists of nematic layers with different direction vector. So cholesteric phase can be referred as helically twisted nematic phase, which is shown in Figure 1.9 b). Cholesterics has no long-range orientation order and no long-range order in positions of the centers of mass of molecules. The arrangement of molecules is quite what one would obtain by twisting about the x axis a nematic initially aligned along the y axis, shown in Figure 1.9 b [29], [30].

Smectic liquid crystals: Both location and orientational order is exist in this phase. Smectic phase has three different types called as A, B and C [30].

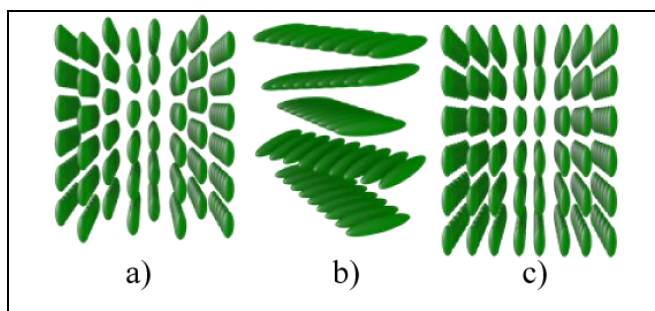


Figure 1.10: Schematic illustration of nematic a), cholesteric b), smectic c) phase of liquid crystals.

- Side Chain Liquid Crystals - Poly (Cholesteryl n-methacryloxybutyrate-co- methyl methacrylate) (Poly (chol-n-MMA-co-MMA)) and Poly (Cholesteryl n-methacryloxybutyrate) (Poly (chol- n-MMA))

In this study PMMA derivatives of side chain liquid crystalline homo-polymers and copolymers are investigated as an alternating dielectric layer for OFET applications to PMMA. These polymers are found as broken focal-conic fan texture of smectic phase.

Side chain liquid crystals demonstrate both properties of polymer and liquid crystalline, which are formed by attaching polymer as side chain. These materials can be varies due to their backbone, aliphatic spacer length and also mesogen. Figure 1.11 is showing desired structure of prepared OFET for this study.

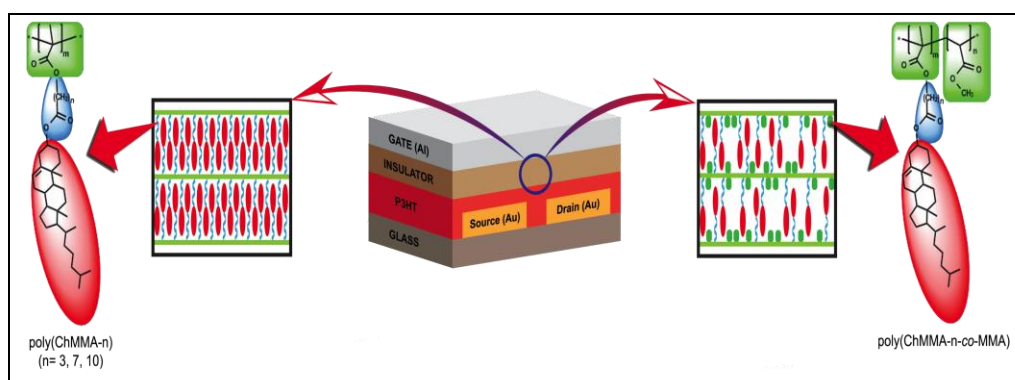


Figure 1.11: Schematic illustration of OFET with SCLCP dielectric layer.

2. DIELECTRIC THEORY and OFET

2.1. Dielectric Theory

A capacitor is a device that stores electric charge. Capacitors can vary in shape and size, but the basic architecture can be explained as, two electrodes carrying equal but opposite charges when there is an applied field. Parallel plate capacitor is the simplest structure to understand capacity phenomena where it is demonstrated in Figure 2.1.

It is proved that charges stored in a capacitor (Q) are linearly proportional to potential (V). This ratio of Q and V gives capacity (C).

$$Q = C|\Delta V| \quad (2.1)$$

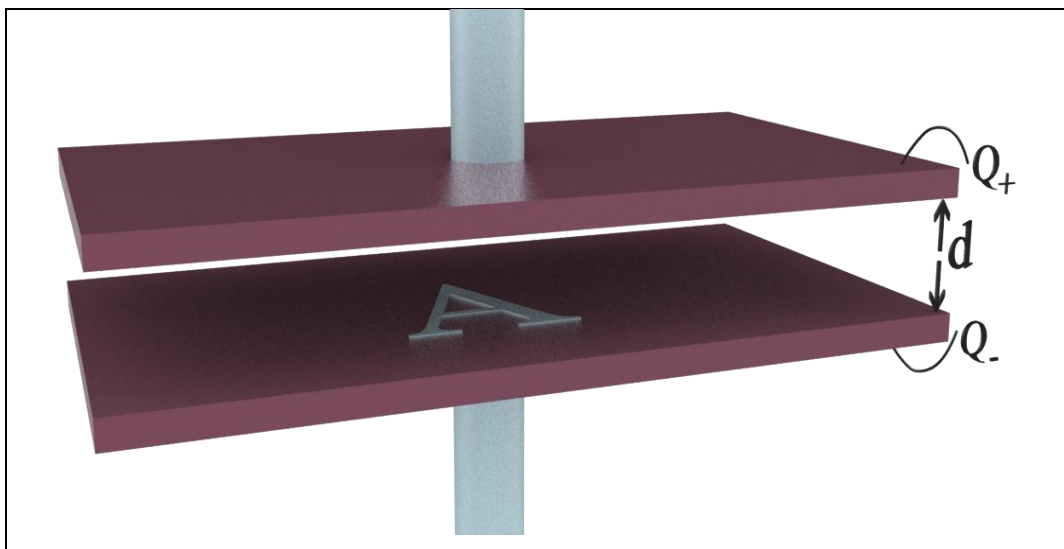


Figure 2.1: Parallel plate capacitor.

2.1.1. Dielectrics

Dielectrics are electrical insulators that can be polarized by an applied electric field. When a dielectric is placed in an electric field, electric charges do not flow through the material, in other words it does not behave as electrically conductor

materials, but it shows only slightly shift from their average equilibrium positions causing dielectric polarization. Dielectrics can be used as electrical insulators in cables or can be used as a cover for electronic devices, which has low dielectric constant. Relatively high dielectric constant materials are using for capacitive applications. As it is mentioned above dielectrics are polarized in electrical field. Polarization due to applied electrical field can be summarized by figure out Clausius– Mossotti equation.

$$P = \frac{\epsilon_r - 1}{\epsilon_r + 2} \times \frac{M}{\rho} = \frac{N_A \alpha}{3 \epsilon_0} \quad (2.2)$$

ϵ_r is the relative permittivity, ϵ_0 is the permittivity in vacuum, M is molecular weight of a repeat unit, ρ is density, P is polarisability, N_A is the Avogadro constant. This equation is the proof of dependency of dielectric constant to polarisability and free volume of the constituents' element present in the materials. Polarisability refer to the proportionality constant for the formation of dipole under the influence of electric field [31].

2.1.2. Dielectric Parameters

Polarization: Many molecules have permanent dipole in its own system, and they annihilate each other so that summation of dipole moment is equal to zero. Figure 2.2 shows that there is no net polarization. When a potential applied to two conductor plates, opposite charges will accumulate at the surface of plates, given in Figure 2.2. Degree of polarization is proportional to applied electric field and can be tunable.

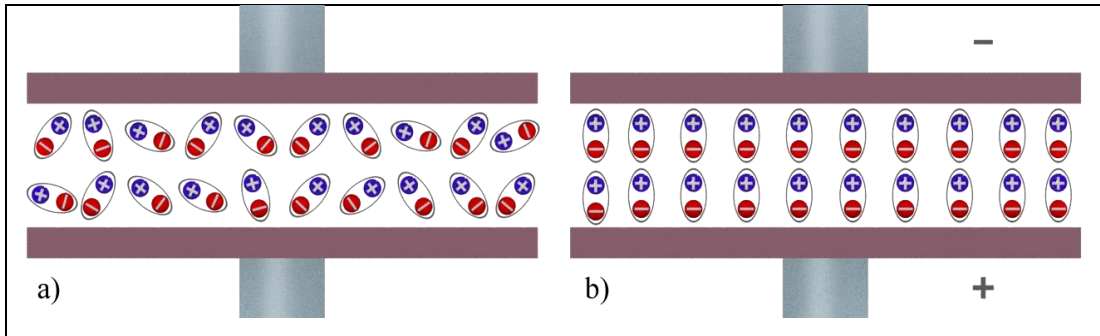


Figure 2.2: a) Dielectric material without orientation between two parallel plates b) Orientational polarization due to applied electric field.

Three different frequency-dependent polarization mechanisms are given in Figure 2.3. At frequency range 10^2 - 10^{10} orientational polarization, at 10^{10} - 10^{13} atomic polarizations and between 10^{13} and 10^{16} electronic polarization could be observed, which could be seen in Figure 2.3 [32].

- i) Electronic polarization is according to the displacement of electrons with respect to the nucleus.
- ii) Atomic polarization is distortion of atomic position in a molecule or lattice.
- iii) Orientational polarization is valid for polar molecules; there is a tendency for permanent dipole to align by the electric field to give a net polarization in that direction [31].

Dielectric relaxations at lower frequency regions (i.e. 100Hz-1MHz) give plenty of information about polar groups and molecular motion [33].

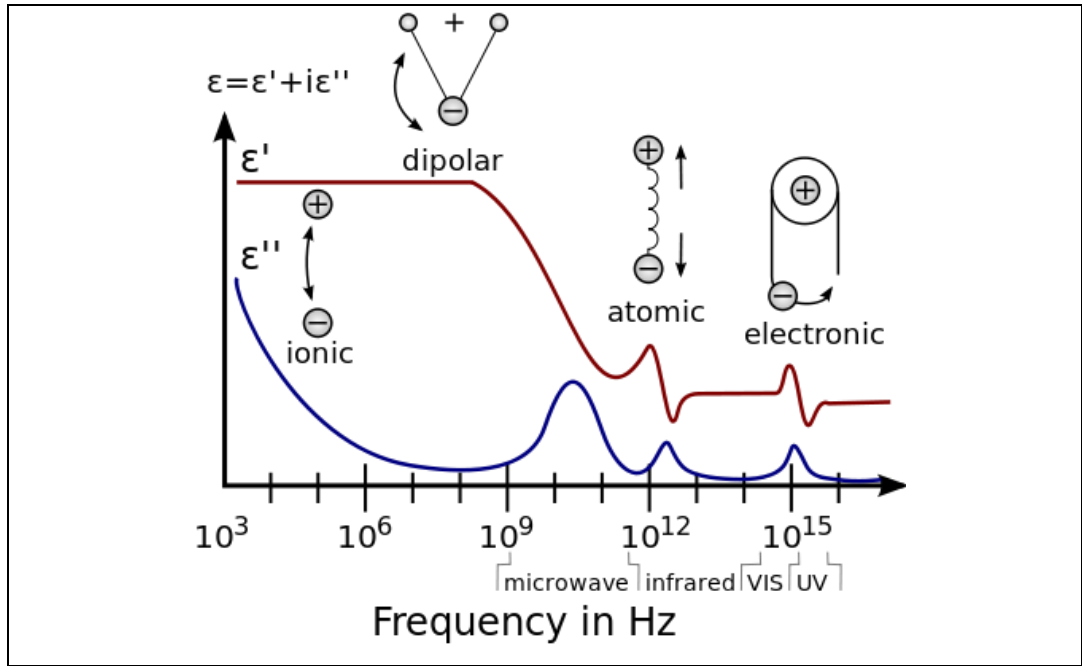


Figure 2.3: Representation of frequency dependent relaxation mechanisms in polar dielectric materials.

Debye (1927) created those dielectric relaxation phenomena, which is the dispersion of the real permittivity (ϵ') and the existence of dielectric absorption (ϵ'') in the phasor domain for dipolar liquids and solids, was according to the reorientational fluctuations of the molecular dipoles. Many dielectric studies followed, particularly those by Smyth (Princeton) and Cole (Brown) that were examined in the 1930s [32].

- Dielectric Constant (Permittivity)

Polarization depends on not only \mathbf{E} but also susceptibility of the dielectric. Every material has its own characteristic storage capacity of energy, which is associated with permittivity. Where permittivity is how a dielectric resist to an applied field. This is proportional to dielectric constant of each material, which is given below equations.

$$\mathbf{P} = \chi\mathbf{E}, \tag{2.3}$$

$$C = \frac{Q}{|\Delta V|} = \frac{\epsilon_0 \epsilon A}{d}, \quad (2.4)$$

Capacity is vary due to the material between two parallel plates, thickness of dielectric film and area of electrodes, which is expressed by the Equation (2.4). Moreover, it can be accepted that using very thin film (in nanometer range) capacitors will give opportunity to get better capacity in a very small area.

When a fixed frequency is applied to capacitor its dielectric constant and also other dielectric parameters must be stable. While measurement was carried out with variable frequency, complex dielectric constant will describe dielectric constant of sample. Complex dielectric constant is given in Equation (2.5). On the other hand, dielectric parameters are changing with existence of temperature and pressure of environment.

$$\epsilon^*(\omega) = \epsilon'(\omega) - i\epsilon''(\omega) \quad (2.5)$$

For all polar dielectric materials permittivity is between 3 and 9 and imaginary part is nearly zero at lower frequencies. So, complex dielectric constant is almost equal to real part of it. However in higher frequencies (more than 100 Hz) imaginary part of complex dielectric constant will increase. At relaxation time polarization will be almost disappear. On the other hand, for nonpolar dielectric materials permittivity is less than 3 also it is independent from AC [31].

Imaginary part of complex dielectric constant gives information about degradation of polarization due to frequency of alternating current. High imaginary dielectric constant means that high energy loss [34]. Where every peak on frequency dependent graph of ϵ'' define critical frequencies [35].

All materials can be analyzed with different spectroscopic techniques according to its own characteristics. Parallel plate capacitor technique is very suitable for materials, which are solution processed. This technique is not only easy but also very reasonable. In this work, all polymers' dielectric characterization was investigated by using thin film capacitor technique.

- Liquid Crystals Dielectric Measurements

Liquid crystals (LCs) are highly nonlinear optical materials due to their sensitivity, which is activating under slightly low optical fields. Also they are very sensitive to applied electric field, their director axis will reorient. This effects causing the change of refractive index and observations of several interesting properties have been extensively studied so far. Molecular orientation of LC molecules due to applied fields, determines the electro-optical behavior of the system and external effects may cause molecules to reorient by molecular interactions. There are two structure types due to their resultant dielectric behavior. First one is called as positive dielectric anisotropy (p-type) and its dielectric constant along the director axis is larger than that along the axes perpendicular to the director. ϵ is greater than zero in this case. The other type is named as negative dielectric anisotropy (n-type) and ϵ is less than zero. Variation of ϵ with respect to the spot frequencies reveals that LC orientation has p-type property at low frequencies, and as the frequency increases the dielectric anisotropy character shifts to n-type. The measurement of the dielectric relaxation at different frequencies gives information about the dynamics of polar groups and molecular motion [36].

2.1.3. Cole-Cole Plots

Cole cole plots are graphs in which describing materials dielectric behaviors. Cole–Cole curves give useful information about the relaxation mechanism of the cells. Real part of permittivity ϵ' is lying on real axis of plot where as imaginary part of dielectric constant ϵ'' is lying on y axis [33].

- Debye Type Relaxations

If the Cole-Cole plots' semicircles are passing through the origin, plots obey Debye-type dispersion with a distribution of relaxation times. The Cole–Cole plots show a semicircle, this will indicate mono-dispersive nature of the dielectric properties of samples. The complex dielectric dispersion curves are expressed by the Cole–Cole relation [32], [37], [38].

- Non- Debye Type Relaxations

If the Cole-Cole plots centers are lying below the real axis, this is the evidence of non- Debye type relaxation. Fitted Cole-Cole plot will be observed as depressed semi-circle. Whereas, this explanation should be done according to absorption coefficient values (α) of samples. Curves are indicating non-Debye type behavior, if absorption coefficient is ($0 < \alpha < 1$) [32], [37], [38].

2.2 Organic Field Effect Transistor (OFET)

Organic field effect transistors (OFETs) using organic semiconductors offer potential to be used as large area electronics that gives a great potential for flexible substrates such as radio frequency identification (RFID) tags, chemical sensors, flexible display, photo sensors. The solution processability of such materials is low cost, has high volume production. To perform OFETs, materials ranging from conductors, semiconductors, to insulators different materials are required. As electrodes, Al, Au, Ag for active channel materials organic semiconductors, especially P3HT, PCBM[39], Pentacene [40], for gate dielectric layers are to insulators SiO₂ [41], PMMA [13], PVA [42].

2.2.1 Basic Device Structure and Physics

Field-effect transistors are three-terminal devices consist of gate, source and drain electrodes. Well-known OFET design can be defined as; an organic semiconductor is deposited as charge carrier channel, the source and drain ohmic contacts, and is itself apart from the gate electrode by one or more insulating gate dielectric layer [43]. Dielectric layer can be both organic and inorganic material [28]. Because of the reasons that has mentioned in the previous chapters, organic dielectric films is investigated in this work. The organic semiconductor and gate dielectric can be deposited by solution processing methods for instance; spin coating, role to role, doctor blading etc.

Schematically illustration of OFET energy levels is given in Figure 3.1. Figure 3.1 indicating basic state for V_{DS} and V_{GS} is zero. Gate voltage can be controlled

according to the intrinsic properties of dielectric layer and semiconductor channel. Due to applied gate voltage polar dielectric material will be polarized, at the interface. This polarization is the reason of induced free charge carriers at the gate dielectric-semiconductor interface. The properties of the active semiconducting organic material layer are changed as seen in a shift of the energy levels in Figure 2.4. By controlling the voltage on the gate, a charge can be induced on the other electrodes [10], [43].

Due to work function of source metal and intrinsic polarization properties of dielectric material certain amount of carrier is flown from source to semiconducting channel hereby, conducting channel will be formed [43], [44].

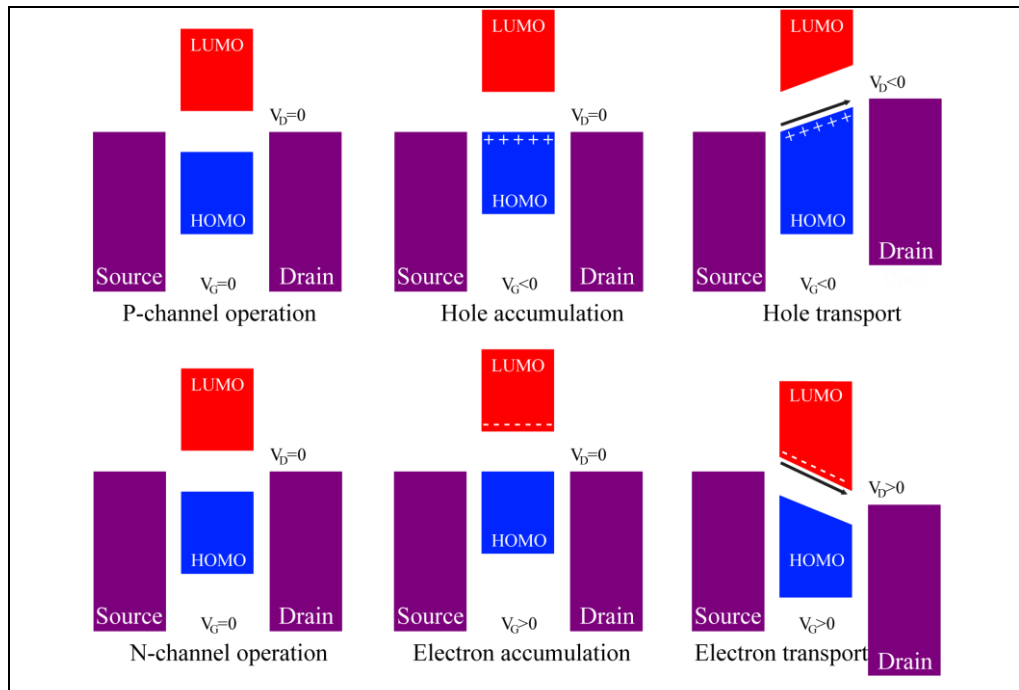


Figure 2.4: The schematic illustration of OFET band structure with a) P-type organic semiconductor b) N-type organic semiconductor.

The gate-voltage dependent shift of energy states enable injection of free charge carriers from the source electrode by accumulating charge carriers in the organic semiconductor. These charges are drifted from the source electrode and collected across the conducting channel at the drain by applying a voltage between the two electrodes.

As given in Figure 2.4 each unipolar class of semiconductor (n and p type) responds to the gate induced field by accumulation of carriers (accumulation voltage), when applying the opposite field a depletion of carriers is observed (depletion voltage). Exclusively the first few molecular layers at the interface to the dielectric material have a high charge carrier density. A conductive channel arises and current can flow from source to drain in consequence of a field is applied across the channel region.

2.2.2. Charge Transport

To understand charge transport mechanism schematic demonstration of an OFET must be investigated. Figure 2.5 is showing channel length and channel width of an OFET where, charge transport in OFETs is formed within 1–2 nanometers of the semiconductor-dielectric interface layer in channel width [45].

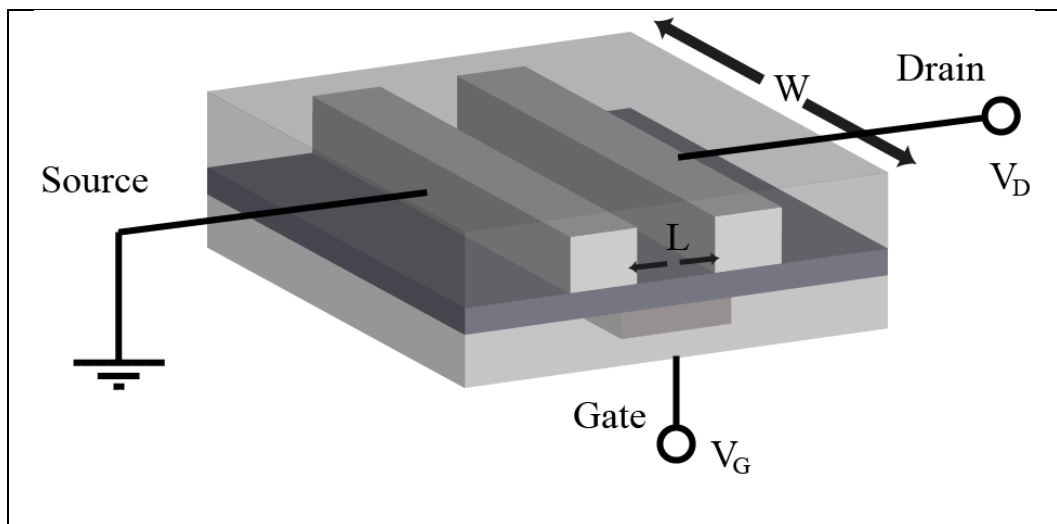
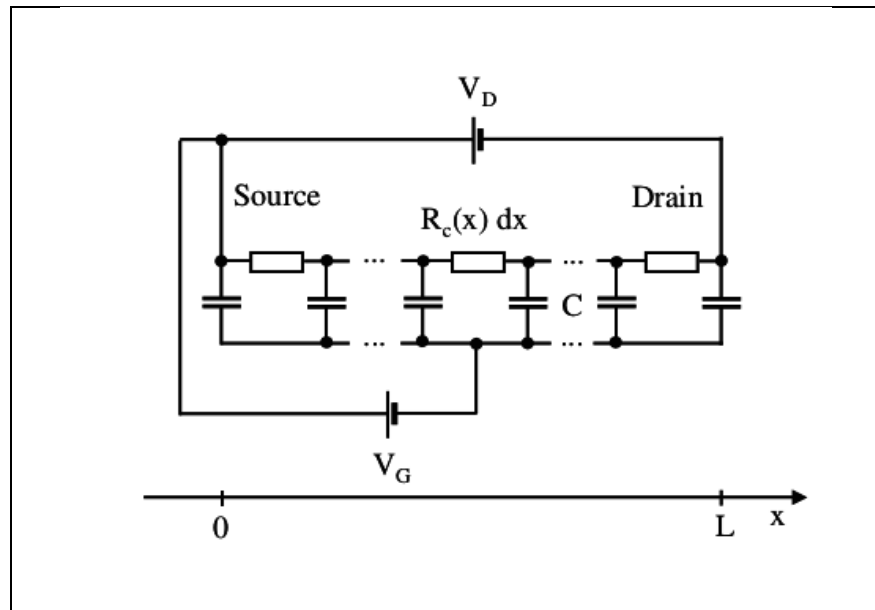


Figure 2.5: Demonstration of channel length and channel width of OFET.

Simple capacitor-resistor-equivalent circuit should be investigated to understand electrical model of a field effect transistor. Figure 2.5 is demonstrating equivalent circuit model of FET that is also valid for OFET. Here R_C is channel resistance, which is equivalent to accumulated charge between source and drain contacts. The extended Shockley equation is defining the FET current-voltage characteristic. V_D and V_G are applied voltage with respect to grounded source

contact. Where V_{DS} is the drain–source voltage, V_{GS} stands for the gate–source voltage and $V_{th,n}$, $V_{th,p}$ express the threshold voltage for electrons and holes respectively. The extended Shockley equation is given in expressions for three different ranges here formulated for the electron accumulation ($V_{GS} > 0$) [46]. The output characteristic shifts to higher current while applying different gate voltage, in case of the accumulation region and to lower current in the event of the depletion region. Typical output characteristics are shown in Figure 2.7 for the case of the accumulation regime. There are two regions in the output characteristics, for a low drain voltage which is called linear region and for high drain voltage which is called saturation region. Most of the output parameters can be extracted from the transfer characteristic (in Figure 2.7), where the drain voltage is constant while the source contact is grounded, and the drain current is measured with respect to the gate voltage [43].



Şekil 2.6: Equivalent circuit model of an OFET.

For $V_D \leq V_G - V_{th,n}$ (unipolar range),

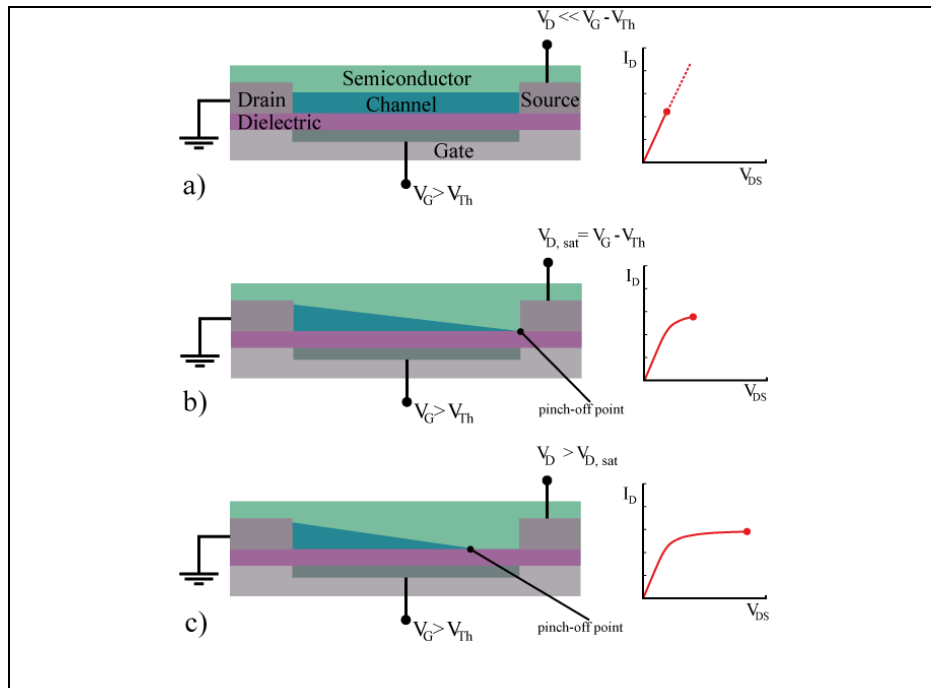
$$|I_{DS}| = \frac{WC}{L} \mu_n \left[(V_{GS} - V_{th,n}) - \frac{1}{2} V_{DS} \right] V_{DS}, \quad (2.6)$$

For $V_{DS} \geq V_{GS} - V_{th,n}$ but $V_{DS} \leq V_{GS} - V_{th,p}$ (saturation range),

$$|I_D| = \frac{WC}{2L} \mu_n [(V_{GS} - V_{th,n})^2], \quad (2.7)$$

For $V_D \geq V_G - V_{th,p}$ (ambipolar range),

$$|I_D| = \frac{WC}{2L} \left[\mu_n (V_{GS} - V_{th,n})^2 + \mu_p [(V_{DS} - (V_{GS} - V_{th,n}))^2] \right]. \quad (2.8)$$



Şekil 2.7: a), b) and c) are schemetic illustration of operation modes of OFET.

Charge transport can occur in organic semiconductors in two ways; first one is charge carrier along the molecule (easy) second is charge carrier along the molecules (this is relatively difficult). Charge carrier is supplied with hopping mechanism in such systems.

Charge transport mechanism of OFETs can be understandable by investigating the properties of this embedded interface, such as its roughness, defect and trap density, and orientation and inter-chain packing of the OFET molecules or macromolecules. To optimize the properties of this interfacial layer will provide the key to future advances in the performance of OFETs [47].

One possible explanation for the enhancement of field effect mobility is the increasing of grain size of the semiconductor.

2.2.3. Current Voltage Characteristics

Two voltages are applied the drain voltage (V_{DS}) is applied to the drain electrode, whereas the source electrode is grounded (0 V), while the gate voltage (V_{GS}) is applied to the gate electrode. Due to channel semiconductor (p-channel or n-channel) OFET characteristics are being measured, the V_{DS} and V_{GS} are given in the negative or positive voltages to accumulate the appropriate sign of charge carriers at the semiconductor-dielectric interface.

The measured field-effect characteristics of these devices can then be classified as transfer characteristics and output characteristics depending on whether V_{GS} is varied while V_{DS} is kept constant, or V_{DS} is varied while V_{GS} is kept constant [44]. These characteristics are typically measured on a semiconductor parameter analyzer (Keitley 4200), and sometimes as a function of temperature, pressure and humidity to understand the underlying physics and sensing parameters of fabricated device. We can easily suppose that using dielectric film with respectively higher dielectric constant will decrease working gate voltage. On the other hand using thin films will provide higher capacity with low gate voltages, which is very promising for using organic dielectric layer.

Examples of transfer and output characteristics are given in Figure 2.8 and Figure 2.9 respectively.

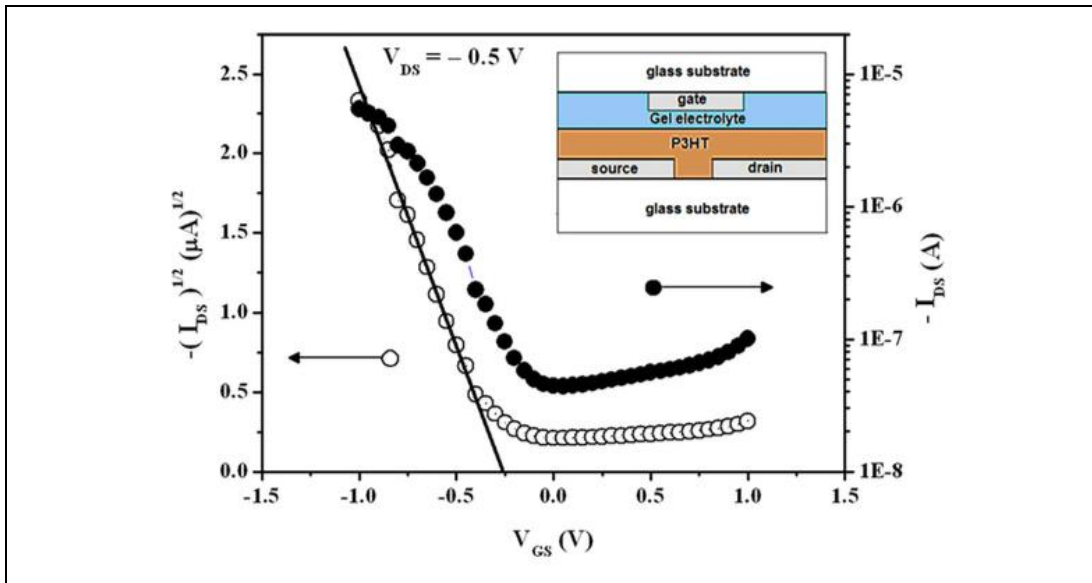


Figure 2.8: Typical transfer characteristics of a polymer OFET.

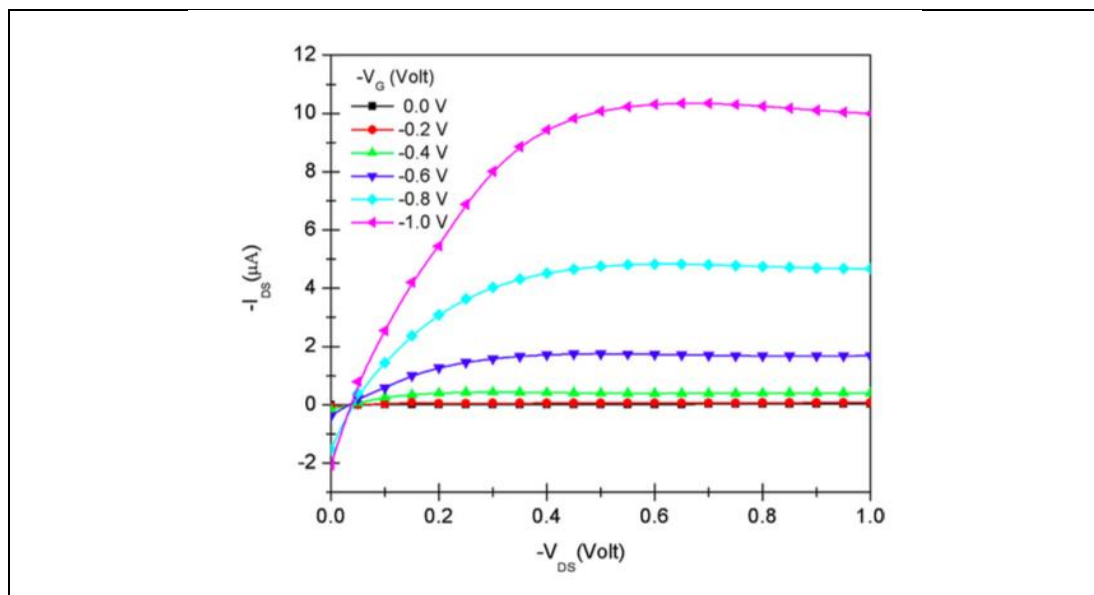


Figure 2.9: Output characteristics of the same polymer OFET.

In the transfer curves, as the magnitude of V_{GS} increases for a given V_{DS} , the source–drain current at first increases quadratically with V_{GS} beyond a threshold voltage, and then quasi-linearly with V_{GS} as V_{GS} becomes larger than V_{DS} . In this

$V_{GS} > V_{DS}$ regime, the linear-regime field-effect mobility (μ_{FET}) can be evaluated using a standard equation from silicon metal-oxide-semiconductor FET theory. In the output curves, as the magnitude of V_{DS} increases for a given V_{GS} , the source–drain current at first increases linearly with V_{DS} , and then levels off, i.e. saturates, as V_{DS} becomes larger than V_{GS} . In this $V_{DS} > V_{GS}$ regime, the saturation m_{FET} can similarly be evaluated.

Mobility;

$$\mu = \sqrt{\frac{\pi}{2}} \frac{ea^2}{\hbar} \frac{J^2}{\sqrt{E_b}} (kT)^{-3/2} e^{-\frac{E_b}{2kT}}, \quad (2.9)$$

Field dependent mobility;

$$\mu(F) = \mu(0) e^{\frac{q}{kT} \beta \sqrt{F}}. \quad (2.10)$$

- Threshold Voltage

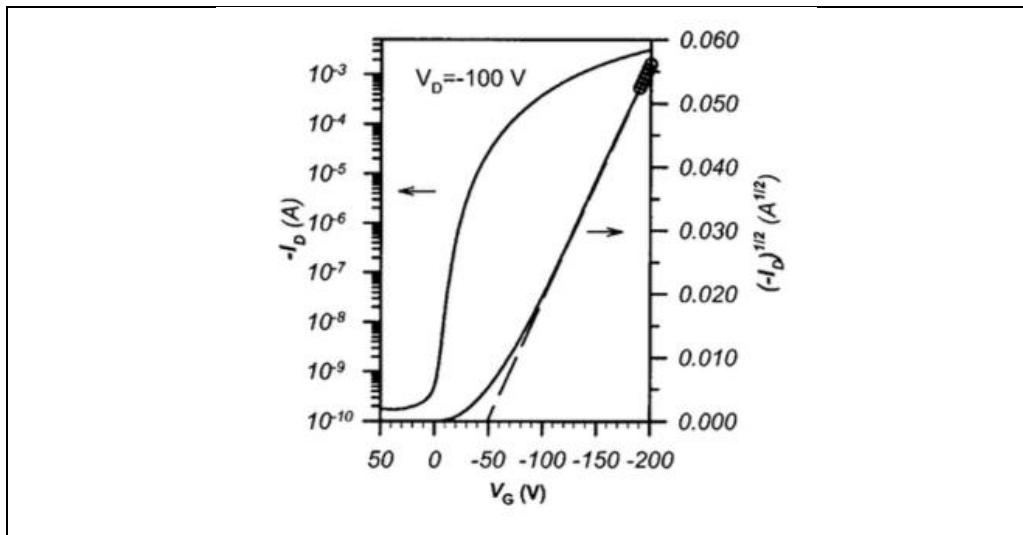


Figure 2.10: Threshold voltage determination of an OFET.

3. MATERIALS and EXPERIMENTAL PART

3.1. Thin Film Capacitor Fabrication

- Substrate

To make thin film capacitor; ITO coated glass was chosen as a substrate. One of the most important factors in a fabrication run is cleaning of the substrates.

ITO coated glass substrates were cleaned by using 10 minutes sequential ultrasonication with acetone, methanol and isopropyl alcohol. The substrates were dried by using argon blow and thermal oven.

- Dielectric Materials

In this work, methacrylate-based side-chain liquid crystalline polymers bearing cholesteryl mesogen was used as gate dielectric. For this reason, these polymers with various lengths of aliphatic spacer were electrically analyzed by using gain/impedance spectrometer. To get better results, investigation of the effect of how molecular weight changes dielectric properties, must be well understood. Various molecular weight of PMMA was analyzed, such as 10k, 50k, 100k, 200k and 500k.

Table 3.1: Investigated dielectric materials.

PMMA samples	Homo-polymers	Co-polymers
PMMA (mw-10k)	Poly(ChMMA-10)	Poly(ChMMA-10-co-MMA)
PMMA (mw-50k)	Poly(ChMMA-7)	Poly(ChMMA-7-co-MMA)
PMMA (mw-100k)	Poly(ChMMA-3)	Poly(ChMMA-3-co-MMA)
PMMA (mw-200k)		Poly(ChMMA-3-co-MMA)% 10
PMMA (mw-500k)		Poly(ChMMA-3-co-MMA) % 5
		Poly(ChMMA-3-co-MMA) % 3
		Poly(ChMMA-3-co-MMA) % 2
		Poly(ChMMA-3-co-MMA) % 1
		Poly(ChMMA-3-co-MMA) % 0.5

PMMA thin films were prepared by using solution-processing method. Solutions were prepared according to molecular weight of samples to prepare smooth and optimum thin films. Solution ratios are given in Table 3.2.

Table 3.2: Solution ratios of PMMA samples.

Molecular Weight of PMMA	Solvent (Toluene)	PMMA
10k	1ml	120mg
50k	1ml	100mg
100k	1ml	80mg
200k	1ml	50mg
500k	1ml	30mg

All PMMA solutions were deposited on ITO coated glasses with spin coating at 2000 rpm for 45 second. Prepared samples were dried in oven, which is given in Figure 3.8, at 110 °C for 15 minutes. Top contacts were chosen as Al, around 100nm.



Figure. 3.1: Thermal oven.

According to molecular weight dependent dielectric result of PMMA new liquid crystals were sensitized by GIT, chemistry department. All of these polymers (poly (chol-n-MMA-co-MMA) and poly (chol-n-MMA)) are obtained from GIT, chemistry department and used without any further process. According to the molecular weight of the sensitized dielectric materials, solution was prepared in toluene (Merck). Solutions were stirred over night at room temperature by using magnetic stirrer. After preparation of solutions, 0.45 μ m filter was used to clear

impurities. ITO coated glasses was spin coated with polymer at 2000 rpm for 2 minutes. Technical drawing of spin coating process is given in Figure 3.2.

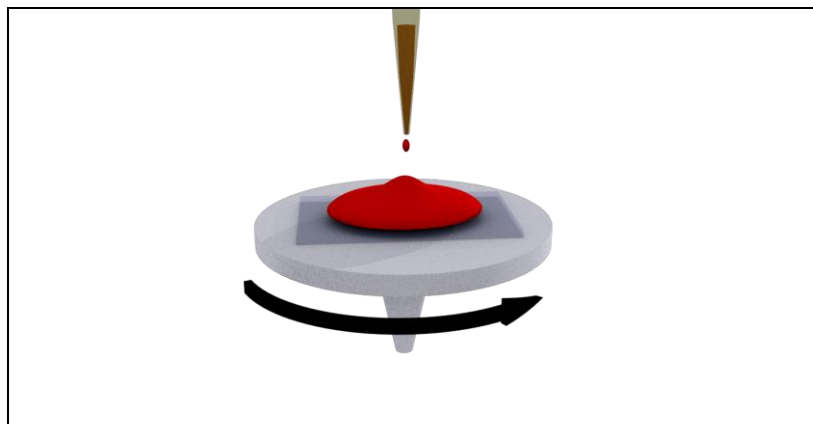


Figure 3.2: Schematically illustration of spin coating process.

Annealing with enforce of heating process is skipped, and thin films was stored in glove box for 12 hours to remove all solvent.



Figure 3.3: Veeco Dektak 8 profilometer.

Dektak 8 profilometer was used to measure accurate thickness of polymer films in GIT, Material Science and Engineering department, related figure is given in Figure 3.3. The polymer films have thickness range from 500nm to 800nm. This thickness measurement had been made to evaluate the accurate static dielectric constant and capacitance.



Figure 3.4: Leybold Thermal Evaporator.

Finally, Leybold thermal evaporator, which is demonstrated in Figure 3.4, was used to coat 50 nm Al film at 10^{-6} mbar. Al and ITO films were designed as electrode. Finally parallel plate type thin film capacitor, were ready to investigate electrical properties of polymers. Technical drawing of prepared capacitors are given in Figure 3.4.

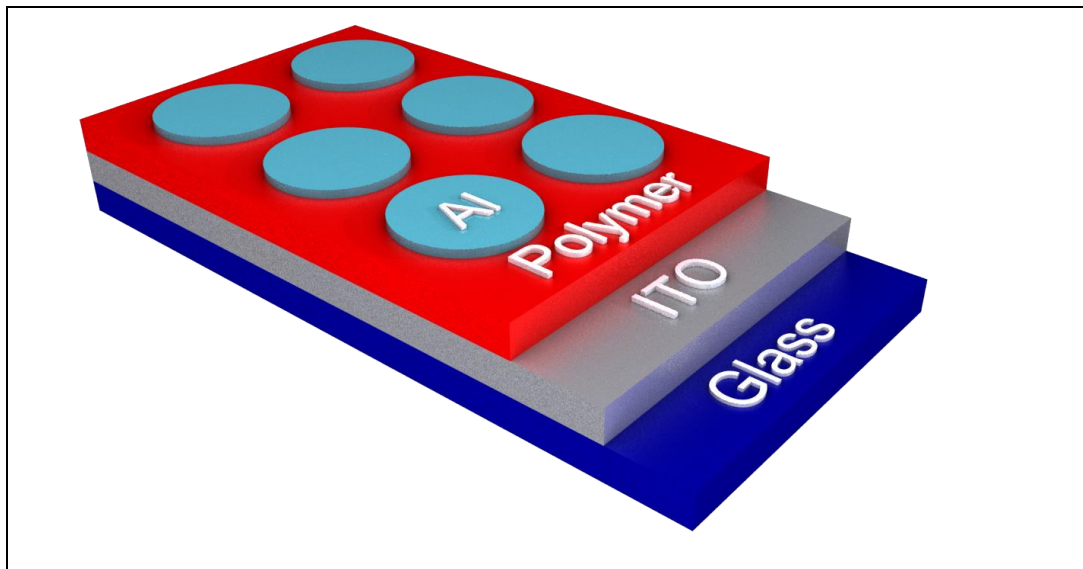


Figure 3.5: Thin film capacitor.

3.2. Spectroscopic Analysis of Polymeric Thin Films

Electrical analyses of thin film capacitors have been applied by using HP 4194A Gain/Impedance analyzer, given in Figure 3.6. Relaxation conditions of polymeric thin films were investigated at 100Hz-15MHz with dielectric analysis. A signal of 1 V peak to peak was applied to the samples during these measurements. All the measurements were performed in the ambient conditions. Real and imaginary parts of dielectric constants, dielectric strength, extinction coefficient, relaxation time and critical frequency all samples were examined. As a result, better dielectric material was chosen to perform desired OFET. Dielectric material was selected due to its high dielectric constant, fast response time and interface properties for OFET fabrication.



Figure 3.6: HP 4194 A Gain/Impedance Analyzer.

3.3. OFET Fabrication

For the top gate OFET fabrication, glass substrate was chosen. Glass substrate was cleaned with the same process of ITO coated glasses that is already given in previous parts.

Ethyl Acetate was chosen as a gate dielectric solvent, not to damage P3HT film, which was coated onto source, and drain contacts.

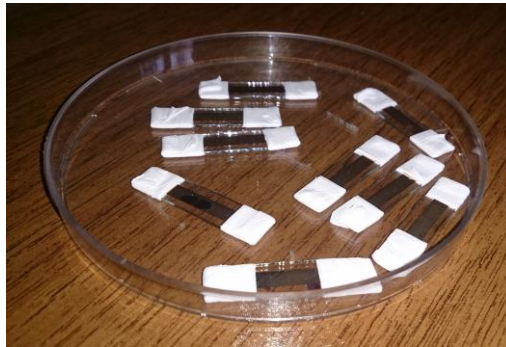


Figure 3.7: Prepared silver source- drain contacts

Top gate/bottom contact OFETs are selected due to dielectric materials properties so that possible interface interaction problem can be solved. This structure is not best but very compatible with flexible surfaces for future application.

As mentioned in previous part glass substrate was firstly cleaned with cleanser detergent, then decontaminated with distil water. Secondly sonication process has done in order of methyl alcohol, acetone, and isopropyl alcohol for ten minutes. All substrates were dried with dry argon gas. Substrates were been prepared for metal contacts. Source drain contacts were applied with thermal evaporation system. Source and drain contact can be both silver and gold. Interaction between contacts and semiconductor layer must be ohmic. For top gate bottom contact devices, source drain layers must be thick. Prepared source drain contacts are given in Figure 3.7.

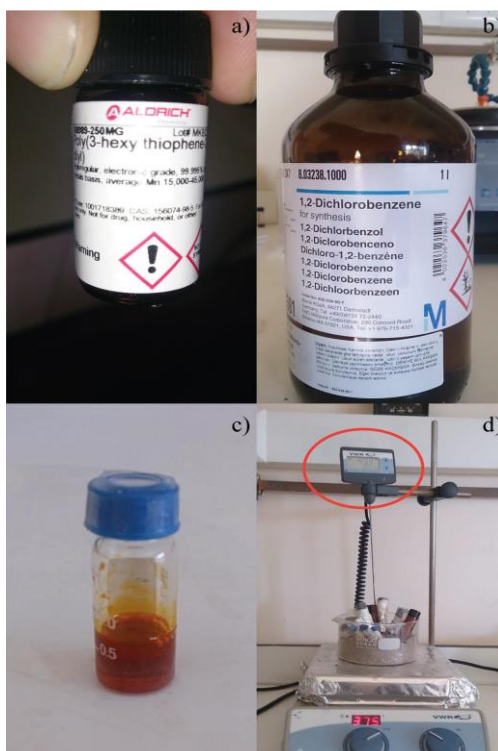


Figure 3.8: Preparation of organic semiconducting polymer (P3HT) solution a) P3HT powder, b) dichlorobenzene, c) P3HT solution and stirring process with magnetic stirrer.

3.3.1. Organic Semiconductor

P3HT is common and very popular organic semiconductor for organic electronics, especially OFET applications with high order of orientation and its high charge carrier mobility range. [48] P3HT was preferred as organic semiconducting layer with its compatibility property with PMMA. P3HT was solved in dichlorobenzene and stirred at 50 °C for 18 hours. Preparation method of P3HT-dichlorobenzene solution is shown in Figure 3.8 due to its preparation process.

All organic semiconductor film was coated with spin coating method. Spin coating method was selected because of its cheapness and easy processing properties. Prepared P3HT films were annealed at 120 °C in glove box ambient for 10 minutes. Dectak 8 profilometer was used to measure P3HT film's thickness. Film thickness is around 300 nm, which is suitable for OFET fabrication.

Then organic semiconductor P3HT was spin coated as designed. On the other hand to get very smooth and clean substrate, glass was directly spin coated with

P3HT at 25 second 500 rpm then 40 second 1000 rpm. After this coating process films were baked at 120 °C in glove box for 10 minutes. Thermally evaporation of source drain can be done after annealing process.

3.3.2. Gate Dielectric

Dielectric material was prepared at room temperature for 12 hours in ethyl acetate solvent. All dielectric films were spun coated at 2000 rpm. Thermal annealing process cannot be applied for such liquid crystal gate dielectrics; device was incubated in glove box for one night. Something never to be forgotten is to get very good interface. Solvent of dielectric should not damage the organic semiconductor film. So that, solvent of dielectric is ethyl acetate which is suitable for P3HT based OFET's. PMMA and Poly(Chol-3-MMA-co MMA) are both used for OFET fabrication process.

3.3.3. Metal Electrode

There exists three types of electrode in a transistor; first one is source, which is grounded, second is drain and last is gate electrode. So that, this is a top gate OFET fabrication, first step is coating source and drain contact with using 50 μm width shadow mask. Silver (Ag) contacts were coated with thermally evaporation system in 10^{-6} mbar. Silver electrode's thickness was planned to be 100-150 nm. For having better bottom contact/top gate OFET thick source –drain contact was desired.

Gate contact Al, was coated on the top of the films with physical vapor deposition technique. One of the most challenging parts of fabrication of top gate OFET is not to perforate dielectric film while evaporating gate electrode. So, gate electrode must not be a heavy metal and also must not evaporate at very high temperatures. To solve all of these problems Al contact was chosen as gate electrode. In this study Al gate have been chosen because of its relatively low melting point. Also, to solve all of this possible problems amount of Al was optimized. 50 mg piece of Al was thermally evaporated through shadow masks. As a result 50 nm gate contacts was obtained.

4. RESULTS

4.1. Dielectric Results

Investigation of electrical characterization gives quite important properties of materials. The real $\epsilon'(\omega)$ and the imaginary $\epsilon''(\omega)$ parts of the complex dielectric constant must be examined for relaxation phenomena, where complex dielectric constant, $\epsilon^*(\omega)$ is defined as given in equation 2.5.

Frequency dependent relaxation mechanism of PMMA was performed to find mostly suitable molecular weight for OFET applications. This pure PMMA samples' measurement is just examined to prove materials are compatible with commercial versions. Relaxation time and real dielectric constants are common proofs of it. It is an expected result that polar molecules give almost stable polarization at lower frequency ($\nu < 10^6$ Hz).

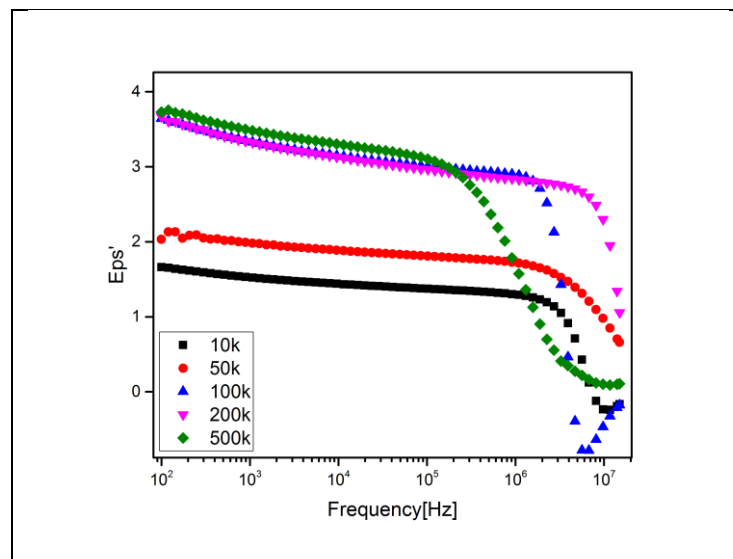


Figure 4.1: Frequency dependent real part of dielectric constant of PMMA homo-polymers with different molecular weight.

Due to results of PMMA with molecular weight 100k is found pretty promising for future OFET applications, which was already taken its place on market. These results are agree with literature and also can be seen in various examples [49].

In the light of this information Poly (Chol-MMA-n) (homo-polymer) and Poly(Chol-MMA-n-co-MMA) (copolymer) were synthesized from PMMA with 100k molecular weight. Their electrical properties were investigated with the same process mentioned in Chapter 3.

The real $\epsilon'(\omega)$ part of the dielectric constant is described as:

$$\epsilon'(\omega) = \epsilon_{\infty} + (\epsilon_s - \epsilon_{\infty}) \frac{1 + (\omega\tau_o)^{1-\alpha} \sin \frac{1}{2} \alpha \pi}{1 + 2(\omega\tau_o)^{1-\alpha} \sin \frac{1}{2} \alpha \pi + (\omega\tau_o)^{2(1-\alpha)}} \quad (4.1)$$

All of the real $\epsilon'(\omega)$ part of homo and copolymers are fitted with Expression 4.1. By fitting real part of dielectric constant we can easily find, extinction coefficient and relaxation time. Imaginer parts of complex dielectric constant will give useful information about critical frequency, which give us chance to understand how accurate is our results (with the comparison of relaxation time). Imaginary part of complex dielectric constants is given in Figure 4.1. Noteworthy variation in the critical frequency of the samples is observed, which is in agreement with the variation of other parameters, which is already illustrated in Table 4.1. Equivalent dielectric constants vary according to the chain length for both homo-polymers and copolymers. From results given real part of complex dielectric constant, it is observed that homo-polymer with chain length 3, (Poly (Chol-MMA-3)) is giving the highest static dielectric constant. Poly (Chol-MMA-3-co-MMA) is ranked as second of all samples. As it is seen from the previous chapters, interface interaction is as important as high dielectric constant of sample. That is why, Poly (Chol-MMA-3-co-MMA) was chosen for OFET applications. To get more information about all samples their imaginer dielectric constant versus frequency, AC conductivity behavior and Cole-Cole plots were also studied as a premise study. In the light of Table 4.1 different LC ratios of (Chol-3-MMA-co-MMA) was sensitized and also examined.

Table 4.1: Absorption coefficient α , relaxation time (τ_0), dielectric parameters (ϵ_s , ϵ_∞ , ϵ''_{max} , and $\Delta\epsilon$) and critical frequencies (f_c) of poly (Chol-n-MMA) and poly (Chol-n-MMA-co-MMA) (n= 3, 7, and 10).

Samples (Adj. R-Square 0.99)	α	τ_0	ϵ_s	ϵ_∞	ϵ''_{max}	$\Delta\epsilon$	$f_c(\text{Hz})$
Poly(Chol-3-MMA-co-MMA)	0.39	7.07×10^{-8}	3.82	-0.10	1.96	3.90	1.31×10^6
Poly(Chol-7-MMA-co-MMA)	0.04	5.80×10^{-8}	2.39	-0.13	1.43	2.42	3.26×10^6
Poly(Chol-10-MMA-co-MMA)	0.27	6.86×10^{-8}	3.25	-0.12	1.66	3.36	2.26×10^6
Poly(Chol-3-MMA)	0.06	5.22×10^{-8}	4.02	-0.30	2.36	4.32	3.91×10^6
Poly(Chol-7-MMA)	0.28	6.64×10^{-8}	2.66	-0.10	1.3	2.76	2.72×10^6
Poly(Chol-10-MMA)	0.74	8.01×10^{-8}	2.85	0.029	1.3	2.82	0.53×10^6

Parameters of Table 4.1 were found according to same measurement method with literature. Here, ϵ_∞ and ϵ_s are highest and lowest angular frequency dielectric constant, $\omega=2\pi$ times the frequency, τ_0 is a generalized relaxation time, and α is the absorption coefficient (also known as extinction coefficient). All of these parameters are found from real dielectric constant versus frequency and imaginary dielectric constant versus frequency plots. The absorption coefficient α parameter changes from zero to one ($0 < \alpha \leq 1$). If $\alpha = 0$, it represents to Debye type relation that means this dielectric is near to ideal dielectric explanation. Where dielectric material shows nearly-Debye type when α value is close to zero and non-Debye type for $0 < \alpha \leq 1$ regions. The calculated values of τ_0 and α are given in Table 4.1. Table shows that α

value is between zero and one, which indicates non-Debye type behavior of samples. It was concluded from results that investigated homo and copolymers obeyed non-Debye and nearly-Debye type relaxation processes.

Table 4.1 also demonstrates the values of parameters ϵ_s , ϵ_∞ and $\Delta\epsilon$. It is observed that these parameters vary due to chain length of different samples. Equivalent dielectric constants vary according to the chain length for both homopolymers and copolymers.

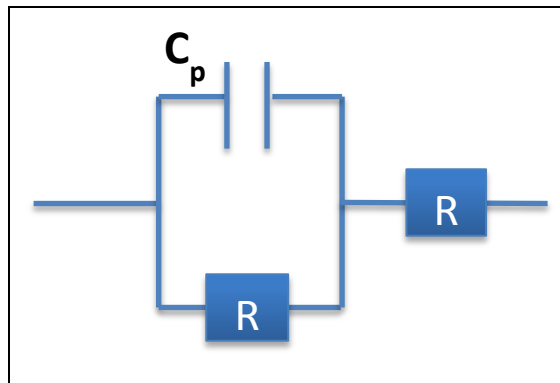


Figure 4.2: Equivalent circuits of thin film capacitors of samples.

The s parameter values can be interpreted by conductivity mechanisms for frequency dependent electrical conductivity mechanisms given in Table 4.2. It is seen that SLPL conduction mechanism at high frequency regions, given in Figure 4.7.

Table 4.2: Definition of conduction mechanism according to s parameter

S parameter	Conductivity mechanism
$s \approx 0$	DC conductivity
$0 < s < 0.7$	Correlated Barrier Hopping (CBH)
$0.7 < s < 1$	Quantum Mechanical Tunelling (QMT)
$1 < s < 2$	Super Linear Power Law (SLPL)

Poly (Chol-7-MMA-co-MMA) polymer is an expectation which gave CBH mechanism at low frequency regions. Furthermore, angular frequency dependent

measurement of Poly (Chol-10-MMA) sample has given three different conductivity mechanisms. The concernment of this sample is, it reaches saturation at high frequencies and parameter s value is almost to zero, DC conductivity like behavior of the sample at higher frequencies, which demonstrate saturation behavior at lower frequencies. That means second polarization occurs after breaking down first polarization. To get better results on OFET applications, understanding of conductivity mechanism is quite important.

To improve dielectric properties of chosen sample, Poly (chol-3-MMA-co-MMA), different dope ratios of LC polymers was investigated, which vary from 10% to 0.5%.

Table 4.3: Absorption coefficient α , relaxation time (τ), dielectric parameters (ϵ_s , ϵ_∞ , ϵ''_{max} , and $\Delta\epsilon$) and critical frequencies (f_c) of poly(Chol-3-MMA-co-MMA) with SCLC ratio 10%, 5%, 3%, 2%, 1% and 0.5%.

Samples (Adj. R-Square 0.99)	α	τ	ϵ_s	ϵ_∞	ϵ''_{max}	$\Delta\epsilon$	$f_c(\text{Hz})$
%0.5	0.68	4.43×10^{-7}	7.06	-0.247	3.13	7.31	2.26×10^6
%1	0.52	1.66×10^{-7}	5.07	-0.157	2.28	5.22	1.88×10^6
%2	0.43	1.22×10^{-7}	4.84	-0.227	2.73	5.06	2.71×10^6
%3	0.52	7.61×10^{-8}	4.01	-0.359	2.66	4.36	4.69×10^6
%5	0.49	5.58×10^{-8}	4.08	-0.244	2.71	4.32	2.72×10^6
%10	0.53	7.14×10^{-7}	4.24	-0.241	2.55	4.45	3.26×10^6

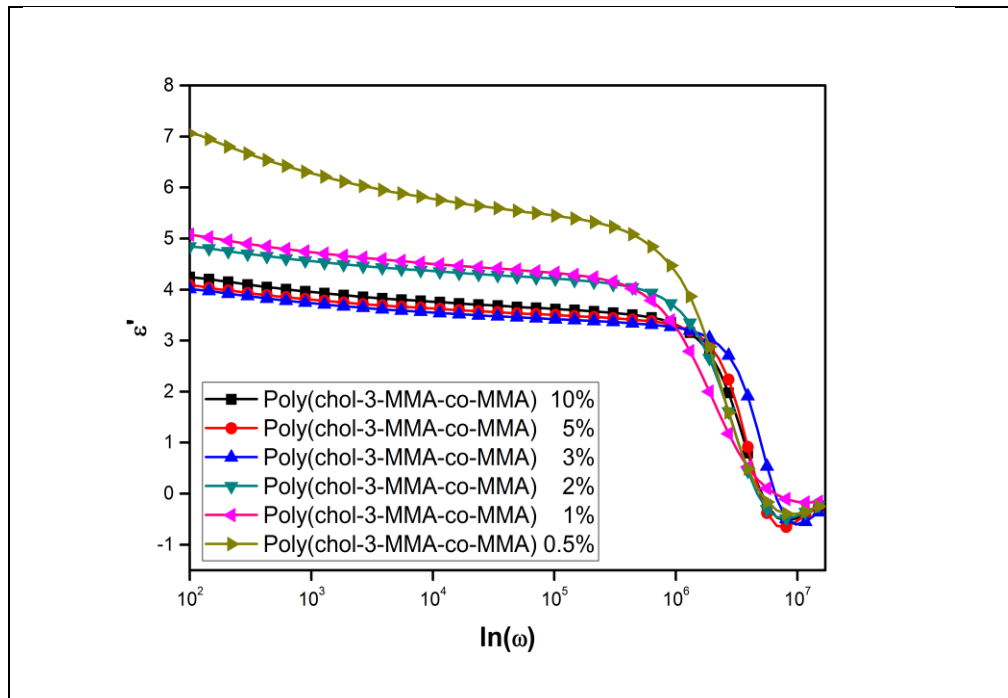


Figure 4.3: Frequency dependent real part of dielectric constant of poly(chol-3-MMA-co-MMA), with SCLC ratio 10%, 5%, 3%, 2%, 1% and 0.5%.

It is clearly seen that values of static dielectric constant of Poly(chol-3-MMA-co-MMA) samples are increasing with decreasing of SCLC ratio. Frequency dependent orientational relaxations are also varying due to SCLC ratio of all samples. The sample with liquid crystal ratio 0.5% is giving the highest static dielectric constant.

Imaginary part of complex dielectric constant is given in Figure 4.4. It can be easily concluded that, static loss factor of poly (chol-3-MMA-co-MMA) 0.5% is the highest, which decrease dielectric strength of material. Critical frequency of all samples again measured by peak values of imaginary part of complex dielectric constant. Match of relaxation time and critical frequency is proved by investigation of two graphs.

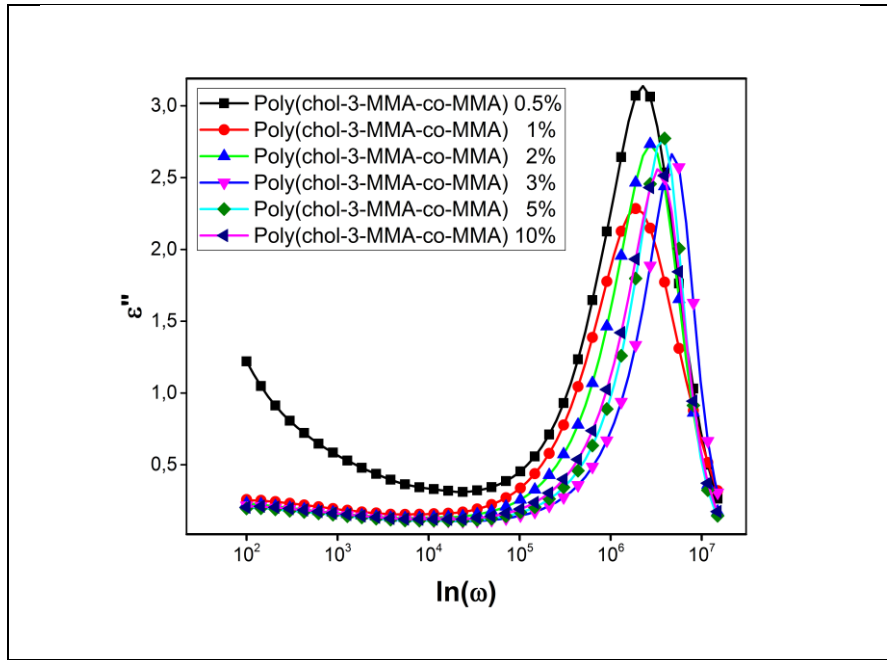


Figure 4. 4: Frequency dependent imaginary part of dielectric constant of poly (chol-3-MMA-co-MMA), with SCLC ratio 10%, 5%, 3%, 2%, 1% and 0.5%.

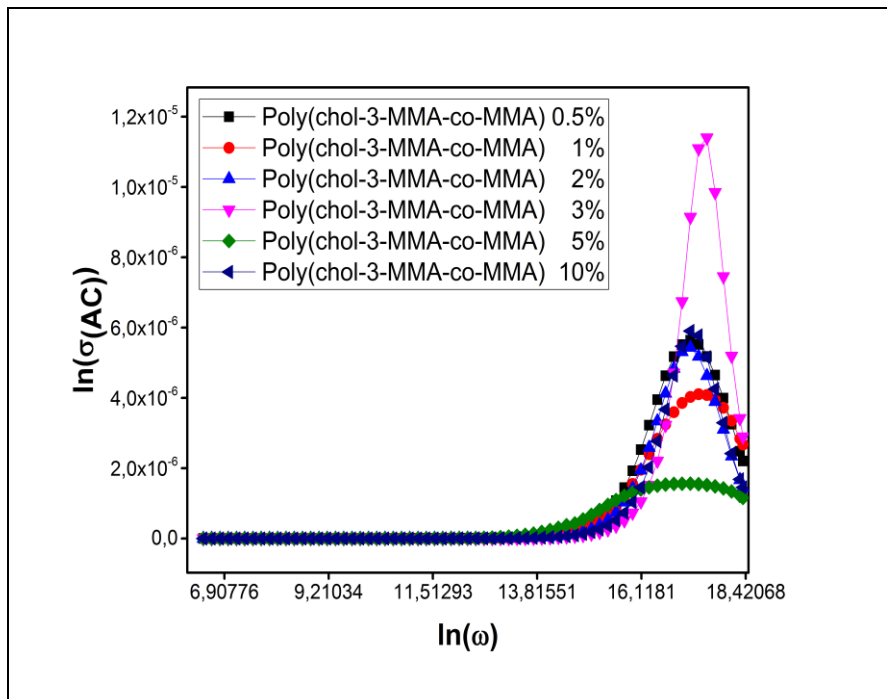


Figure 4.5: Specific conductivity plot of poly (chol-3-MMA-co-MMA), with SCLC ratio 10%, 5%, 3%, 2%, 1% and 0.5%.

Figure 4.5 is demonstrated that, electrical conductivity of all samples is almost zero with low frequency regions. To consider conductivity behaviors of polymers,

separately investigation of graphs are required. Without closer investigation of conductivity behaviors it can be accepted that Poly (chol-3-MMA-co-MMA) 5% give saturation at high frequency region. Closer investigation of Figure 4.5 was again performed to see conduction mechanism. S parameter was found with the same method used above, and graphs are also given in below.

Angular frequency dependent specific conductivity behavior of each sample was investigated to find out conductivity mechanism of them. To investigate exact behavior, we should take a closer look of specific conductivity versus angular frequency plot. To do this, the values of parameter s (angular frequency exponent) were calculated from the slopes of Figure 4.6, Figure 4.7, Figure 4.8, Figure 4.9, Figure 4.10 and Figure 4.11.

All of the fit curves are obtained by using linear equation, $y=a+b*x$, expressing $b=\ln\sigma/\ln\omega$ with R-Square: ~ 0.99 . $\ln\sigma_{AC}$ with angular frequency changes is clearly observed for all samples. Moreover, the s parameter is used to determine the electrical conductivity mechanism for all samples, its values have been figured out from the slopes for each region.

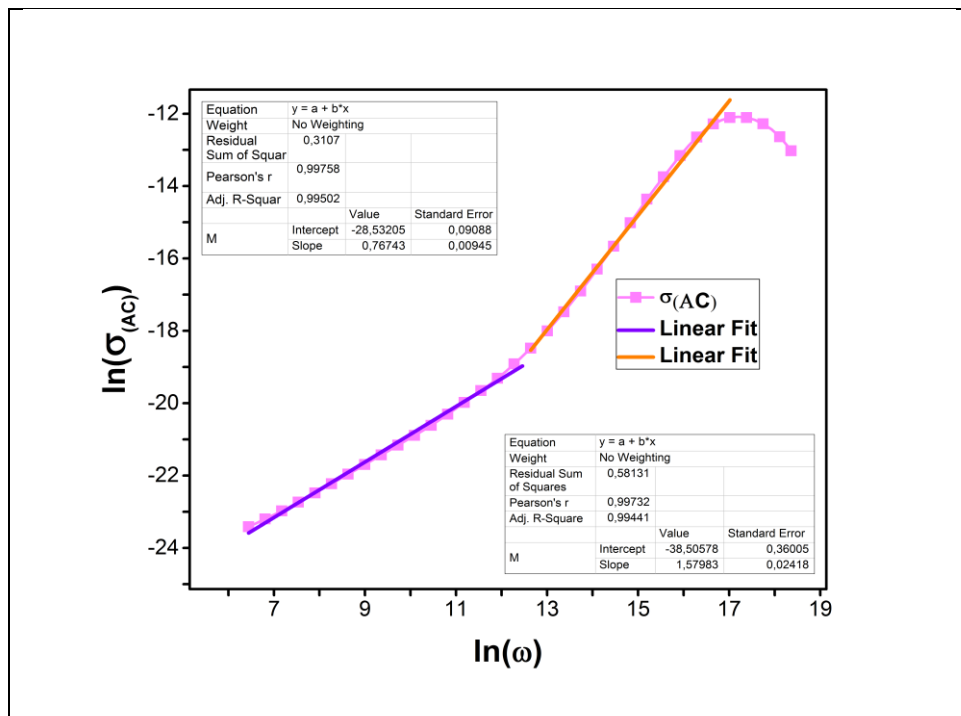


Figure 4.6: Plot of $\ln(\sigma_{AC})$ versus $\ln(\omega)$ of Poly (chol-3-MMA-co-MMA) with SLCL ratio 0.5%.

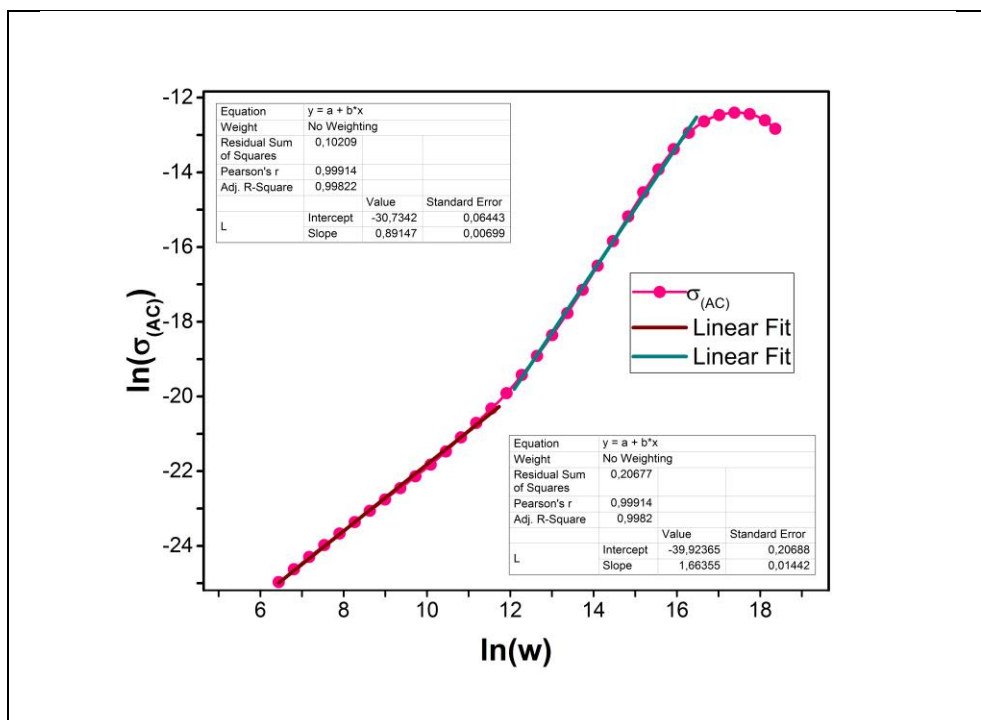


Figure 4.7: Plot of $\ln(\sigma_{(AC)})$ versus $\ln(w)$ of Poly (chol-3-MMA-co-MMA) with SLCL ratio 1%.

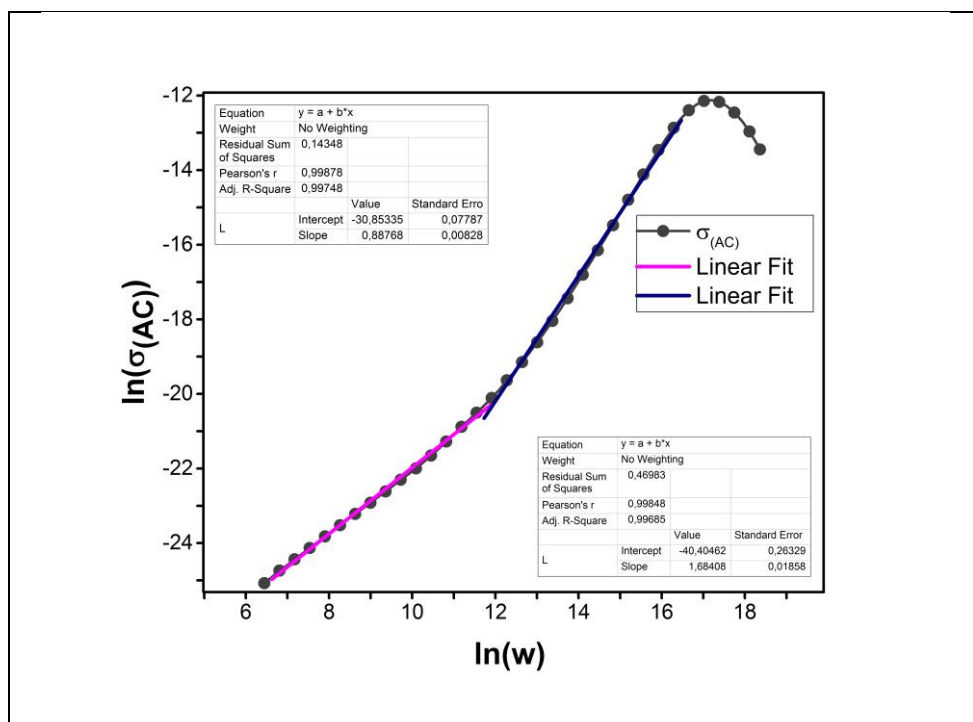


Figure 4.8: Plot of $\ln(\sigma_{(AC)})$ versus $\ln(w)$ of Poly (chol-3-MMA-co-MMA) with SLCL ratio 2%.

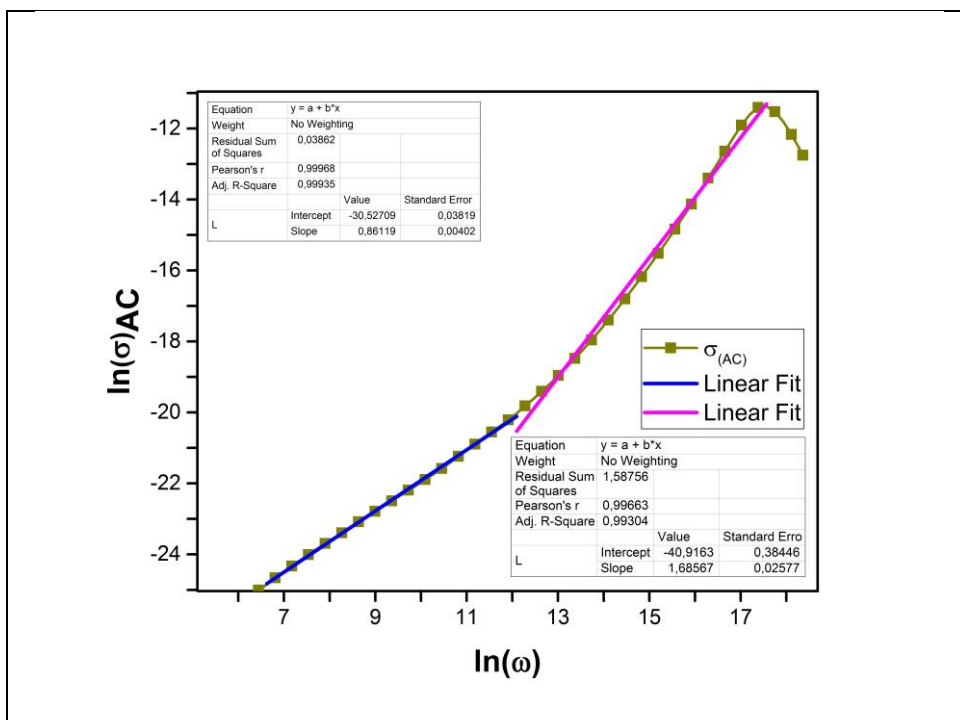


Figure 4.9: Plot of $\ln(\sigma_{(AC)})$ versus $\ln(\omega)$ of Poly (chol-3-MMA-co-MMA) with SLCL ratio 3%.

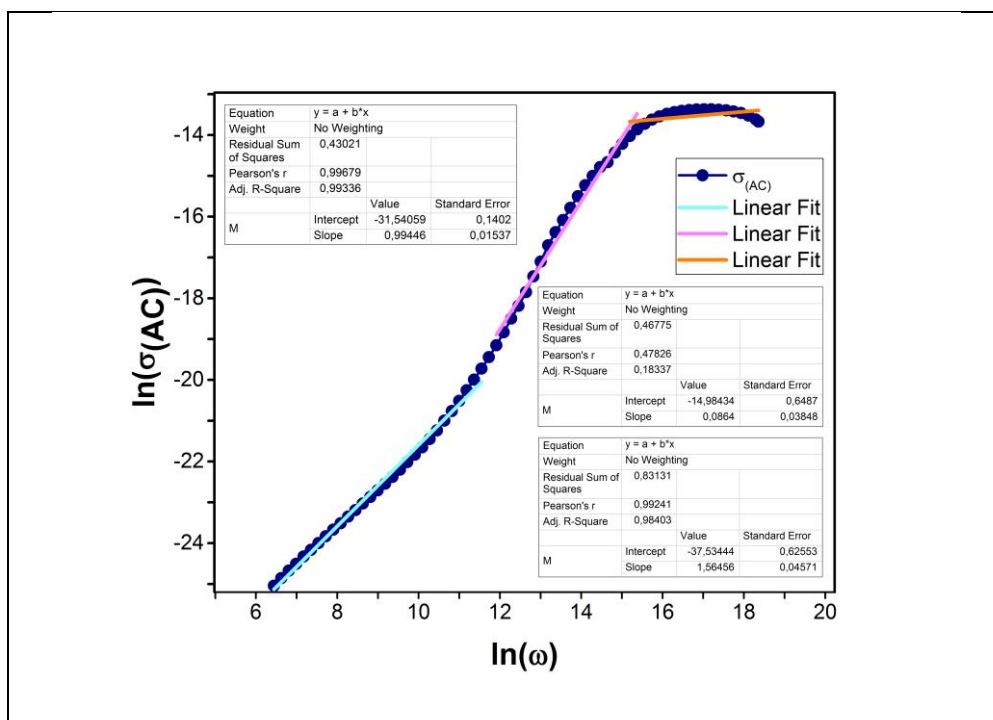


Figure 4.10: Plot of $\ln(\sigma_{(AC)})$ versus $\ln(\omega)$ of Poly (chol-3-MMA-co-MMA) with SLCL ratio 5%.

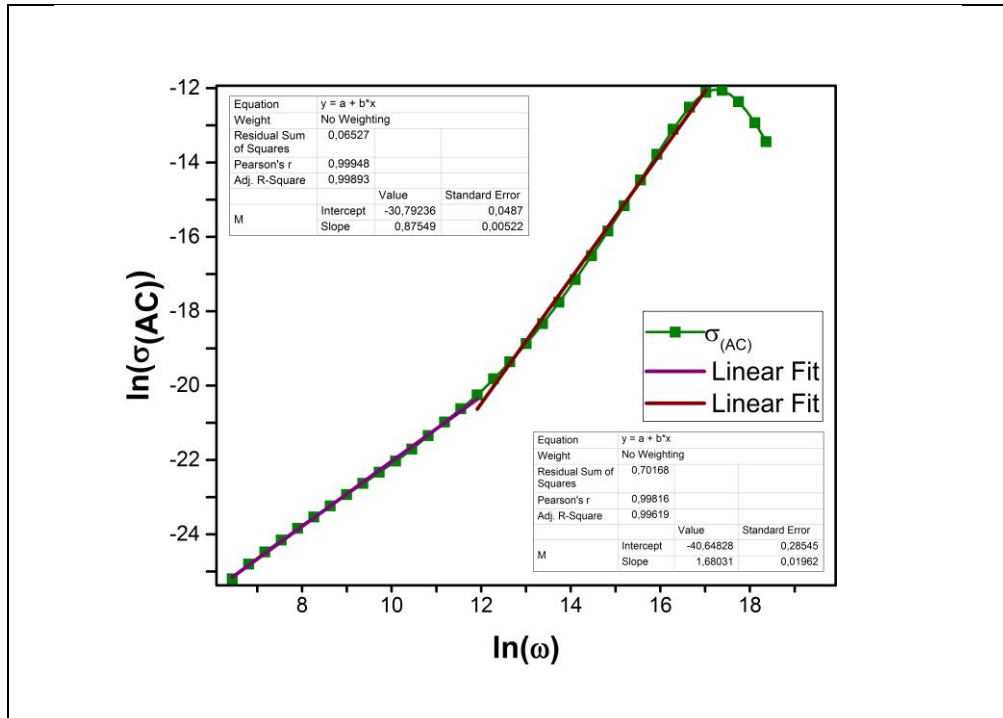


Figure 4.11: Plot of $\ln(\sigma_{(AC)})$ versus $\ln(\omega)$ of Poly (chol-3-MMA-co-MMA) with SLCL ratio 10%.

All polymers, which include SCLC concentration ratios of Poly(chol-3-MMA-co-MMA)'s conduction mechanism is investigated. Nearly all ratios of it (10%, 5%, 3%, 2%, 1%, 0.5%) shows same conductivity mechanism for low and higher frequency regions. It is demonstrated from Figure 4. 6, Figure 4.7, Figure 4.8, Figure 4.9, Figure 4.10 and Figure 4.11, that CBH conduction mechanism was observed at lower frequency regions and SLPL conduction mechanism for higher regions. mechanism gösterdi. Poly(chol-3-MMA-co-MMA) with SCLC ratio 0.5% was given nearly CBH conduction mechanism at lower frequencies. Moreover, Poly(chol-3-MMA-co-MMA) with SCLC ratio 5% gives nearly DC conductivity with s parameter 0.08.

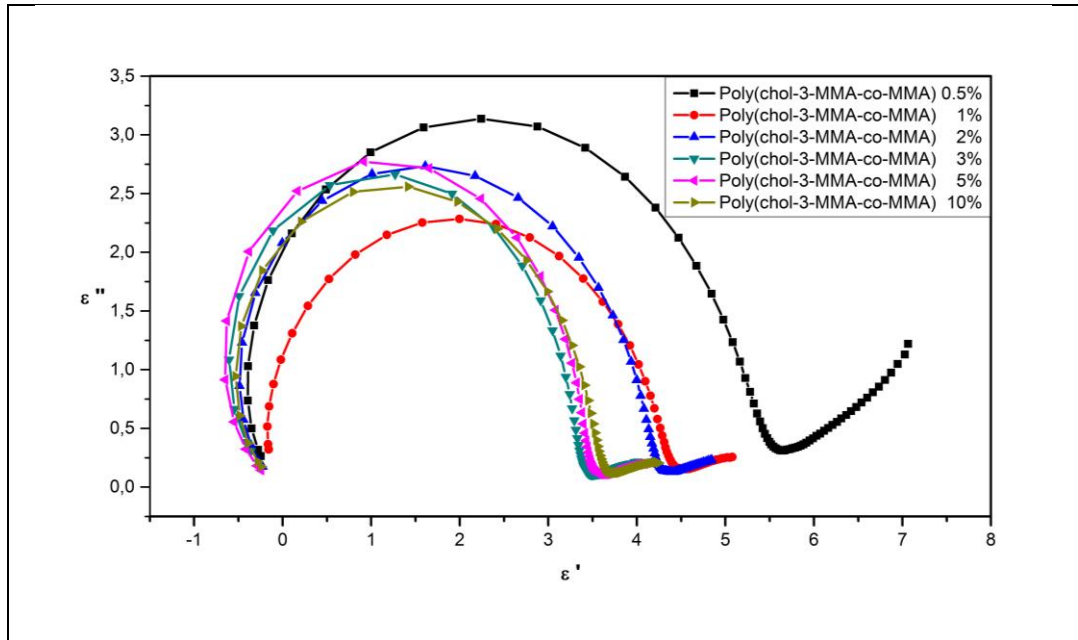


Figure 4.12: Cole-Cole plots of plot of Poly (chol-3-MMA-co-MMA) with SLCL.

Cole–Cole plots was found as parallel Resistance-Capacitance (RC) and series Resistance (R) regimes for the investigated samples. These Cole–Cole plots were obtained from the imaginary versus real values of dielectric constants (ϵ'' – ϵ'). Equivalent circuit model analysis of the Cole–Cole plots show parallel Resistance-Capacitance (RC) and series Resistance (R) regimes for the investigated samples.

4.2 OFET Results

As it was mentioned in chapter 3 output characteristics of fabricated OFET were analyzed immediately by Keitley 4200 SCS at room temperature. V_{DS} was kept at 60V and V_{GS} was swept from -60 to 60 V Current Charges in I_{DS} was observed and investigated. On/Off ratio and threshold voltage were found according to Figure 4.13 and calculated with same procedure in literature. On/Off ratio was founded 2, which was poor but also acceptable result for OFETs in literature.

These challenges can be handle out with optimization and improving interface interactions. Threshold voltage was determined around 6V.

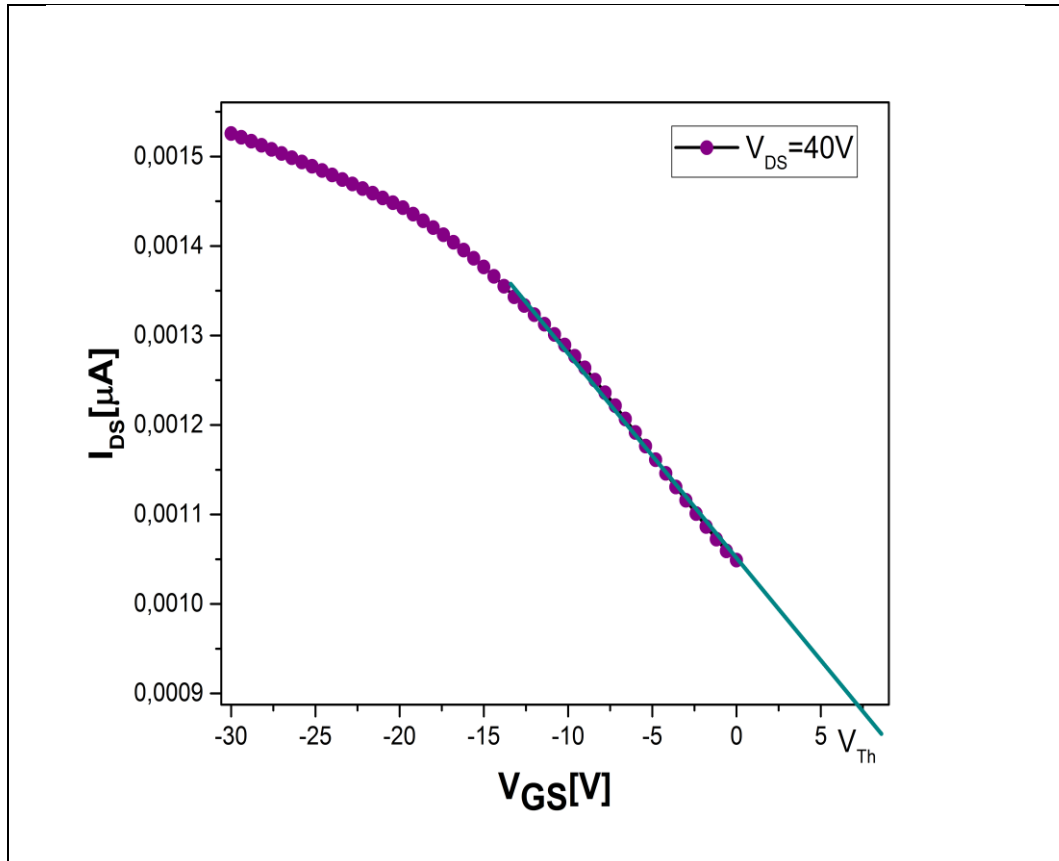


Figure 4.13: Output characteristics of prepared OFET.

Transfer characteristics of fabricated OFET was investigated by step V_{GS} . Figure 4.14 demonstrated that I_{DS} is increasing according to increasing of V_{GS} . Which was a desired result for OFET. It can be easily seen that OFET gives very low saturation behavior in its operation region. V_{GS} dependent increment was again not too much that it gives consistency with output characteristics.

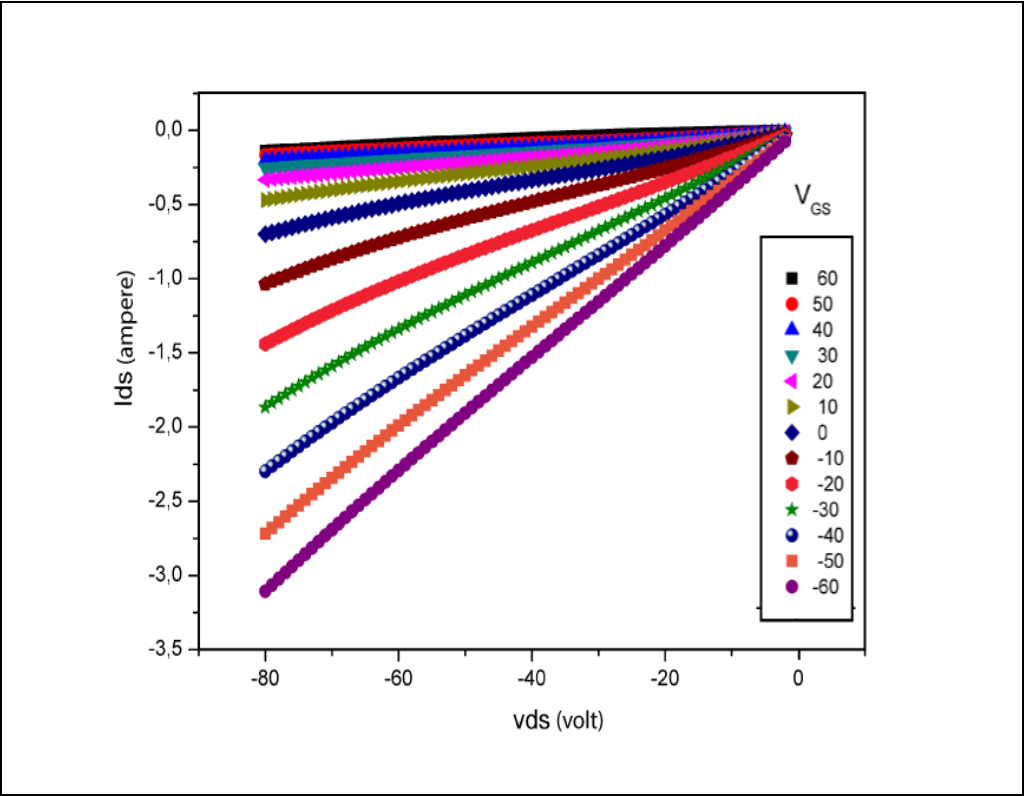


Figure 4.14: Transfer characteristics of fabricated OFET.

5. CONCLUSION

The purpose of this thesis is taking advantage of peculiar properties of liquid crystalline material at electrical field for OFET applications. For this reason, electrical characterization of side chain liquid crystalline polymers is performed. It is seen that side chain liquid crystal polymers with various aliphatic spacer length are given different electrical properties. It is surprisingly concluded that poly (chol-7-MMA-co MMA) could be used for high frequency applications of OPV devices. Poly (chol-3-MMA-co-MMA) was chosen to grow as dielectric layer. It is also observed from experimental results that dielectric constant value is proportionally increased with decreasing the ratio of SCLC polymers. The polymer which includes 0.5% SCLC was selected; it was quite desired result to solve this dielectric polymer in ethyl acetate. Right after the results of dielectric analysis, OFET fabrication was processed. Top gate / bottom contact structure was selected to see its possibility to use in flexible applications. Although it gives low on/off ratio, it is very promising for future application on flexible substrate.

This study can be accepted as a pioneer work for OFET fabrication with using SCLC polymers. Liquid crystalline polymers are quite rewarding for new generation technological devices. Because of its extraordinary behavior on different conditions; temperature, pressure and humidity sensing properties must be investigated in further researches. Moreover OFETs are very desirable with their easy-processing, cheap manufacturing properties. Therefore, OFET with SCLC dielectric layer must be taken into account for sensor manufacturing.

REFERENCES

- [1] Huang Y., Kramer E. J., Heeger A. J., Bazan G. C., (2014), "Bulk Heterojunction Solar Cells: Morphology and Performance Relationships", *Chemical Reviews*, 114(14), 7006-7043.
- [2] Fukuda K., Takeda Y., Yoshimura Y., Shiwaku R., Tran L. T., Sekine T., Mizukami M., Kumaki D., Tokito S., (2014), "Fully-printed high-performance organic thin-film transistors and circuitry on one-micron-thick polymer films", *Nature Communications*, 5, 6016-6024.
- [3] Meager I., Nikolka M., Schroeder B. C., Nielsen C. B., Planells M., Bronstein H., Rumer J. W., James D. I., Ashraf R. S., Sadhanala A., Hayoz P., Flores J.-C., Siringhaus H., McCulloch I., (2014), "Thieno[3,2-b]thiophene Flanked Isoindigo Polymers for High Performance Ambipolar OFET Applications", *Advanced Functional Materials*, 24, 7109-7115.
- [4] Torsi L., Magliulo M., Manoli K., Palazzo G., (2013), "Organic field-effect transistor sensors: a tutorial review", *Chemical Society Reviews*, 42(22), 8612-8628.
- [5] Maddalena F., (2011), "Organic Field-Effect Transistors for Sensing Applications", Doctor of Philosophy Thesis, University of Groningen.
- [6] Klauk H., Halik M., Zschieschang U., Eder F., Schmid G., Dehm C., (2003), "Pentacene organic transistors and ring oscillators on glass and on flexible polymeric substrates", *Applied Physics Letters*, 82(23), 4175.
- [7] Brondijk J. J., (2013), "Device physics of organic field effect transistors", Doctor of Philosophy Thesis, Universitat Groningen.
- [8] Johnson M. T., Zhou G., Zehner R., Amundson K., Henzen A., van de Kamer J., (2005), "56.1: Invited Paper: High Quality Images on Electronic Paper Displays", *SID Symposium Digest of Technical Papers*, 36(1), 1666-1669.
- [9] Kim S. H., Yoon W. M., Jang M., Yang H., Park J.-J., Park C. E., (2012), "Damage-free hybrid encapsulation of organic field-effect transistors to reduce environmental instability", *Journal of Materials Chemistry*, 22(16), 7731-7738.
- [10] Horowitz G., (1998), "Organic Field-Effect Transistors", *Advanced materials*, 10(5), 365-377.
- [11] Jia Z., (2011), "Interfacial Studies in Organic Field-Effect Transistors", Doctor of Philosophy Thesis, Columbia University.
- [12] Hayakawa R. P., Matthieu Chikyow T., Wakayama Y., (2008), "Interface engineering for molecular alignment and device performance of quaterylene thin films", *Applied Physics Letters*, 93(15), 153301-153303.

- [13] Seo J., Park S., Nam S., Kim H., Kim Y., (2013), "Liquid Crystal-on-Organic Field-Effect Transistor Sensory Devices for Perceptive Sensing of Ultralow Intensity Gas Flow Touch", *Scientific Report*, 3, 1-6.
- [14] Kaltenbrunner M., White M. S., Glowacki E. D., Sekitani T., Someya T., Sariciftci N. S., Bauer S., (2012), "Ultrathin and lightweight organic solar cells with high flexibility", *Nature Communication*, 3, 770-780.
- [15] Dai L., (2004) "Intelligent Macromolecules for Smart Devices", *Engineer Materials and Processes*, 1st Edition, Springer London.
- [16] He J., Tallman D. E., Bierwagen G. P., (2004), "Conjugated Polymers for Corrosion Control: Scanning Vibrating Electrode Studies of Polypyrrole-Aluminum Alloy Interactions", *Journal of The Electrochemical Society*, 151(12), B644-B651.
- [17] Smela E., (2003), "Conjugated Polymer Actuators for Biomedical Applications", *Advanced Materials*, 15(6), 481-494.
- [18] Gross M., Muller D. C., Nothofer H.-G., Scherf U., Neher D., Brauchle C., Meerholz K., (2000), "Improving the performance of doped [pi]-conjugated polymers for use in organic light-emitting diodes", *Nature*, 405(6787), 661-665.
- [19] Kim H. J., Han A. R., Cho C.-H., Kang H., Cho H.-H., Lee M. Y., Fréchet J. M. J., Oh J. H., Kim B. J., (2011), "Solvent-Resistant Organic Transistors and Thermally Stable Organic Photovoltaics Based on Cross-linkable Conjugated Polymers", *Chemistry of Materials*, 24(1), 215-221.
- [20] Kymissis I., (2008) "Organic Field Effect Transistors: Theory, Fabrication and Characterization", 1st Edition, Springer.
- [21] Shirakawa H., Louis E. J., MacDiarmid A. G., Chiang C. K., Heeger A. J., (1977), "Synthesis of electrically conducting organic polymers: halogen derivatives of polyacetylene, (CH)", *Journal of the Chemical Society, Chemical Communications*, (16), 578-580.
- [22] Coropceanu V., Cornil J., da Silva Filho D. A., Olivier Y., Silbey R., Brédas J.-L., (2007), "Charge Transport in Organic Semiconductors", *Chemical Reviews*, 107(4), 926-952.
- [23] Bayram G., (2014), "Esnek Nitelikli Organik Güneş Hücresi Yapımı ve Karakterizasyonu", Master of Science Thesis, Gebze Institute of Technology.
- [24] Wang T., Dunbar A. D. F., Staniec P. A., Pearson A. J., Hopkinson P. E., MacDonald J. E., Lilliu S., Pizzey C., Terrill N. J., Donald A. M., Ryan A. J., Jones R. A. L., Lidzey D. G., (2010), "The development of nanoscale morphology in polymer:fullerene photovoltaic blends during solvent casting", *Soft Matter*, 6(17), 4128-4134.
- [25] Basiricò L., (2012), "Inkjet Printing of Organic Transistor Device", Doctor of Philosophy Thesis, University of Cagliari.

- [26] Ali K., Pietsch U., Grigorian S., (2013), "Enhancement of field-effect mobility due to structural ordering in poly(3-hexylthiophene) films by the dip-coating technique", *Journal of Applied Crystallography*, 46(4), 908-911.
- [27] Ha Y.-G., Everaerts K., Hersam M. C., Marks T. J., (2014), "Hybrid Gate Dielectric Materials for Unconventional Electronic Circuitry", *Accounts of Chemical Research*, 47(4), 1019-1028.
- [28] Ortiz R. P., Facchetti A., Marks T. J., (2009), "High-k Organic, Inorganic, and Hybrid Dielectrics for Low-Voltage Organic Field-Effect Transistors", *Chemical Reviews*, 110(1), 205-239.
- [29] Andrienko D., (2006), "Introduction to liquid crystals", 1st Edition, Max Planck Institute, IMPRS school,.
- [30] San S. E., (2002), "Boya Katkılı Nematik Sıvı Kristallerde Optik Nonlinearitenin Kırınım Ağı Difraksiyonu Yöntemi İle İncelenmesi", Doctor of Philosophy, Middle East Technical University.
- [31] Ahmad Z., (2012), "Polymeric Dielectric Materials", 1st Edition, Intech.
- [32] Schönhals F. K. A., (2003) "Broadband Dielectric Spectroscopy", 2nd Edition, Springer.
- [33] Okutan M., Yakuphanoglu F., San S. E., Koysal O., (2005), "Impedance spectroscopy and dielectric anisotropy-type analysis in dye-doped nematic liquid crystals having different preliminary orientations", *Physica B: Condensed Matter*, 368(1-4), 308-317.
- [34] Okutan M., Kavanoz H. B., İçelli O., Yalçın Z., Ay F., Delipınar D., Yakuphanoglu F., (2014), "Dielectric characterization of electro-coagulated boron waste", *Vacuum*, 101 298-300.
- [35] Şengez B., Doğruyol Z., San S. E., Kösemen A., Yılmaz F., Okutan M., Yerli Y., Demir A., Başaran E., (2013), "Use of side chain thiophene containing copolymer as a non-ionic gel-dielectric material for sandwich OFET assembly", *Microelectronic Engineering*, 103, 111-117.
- [36] Okutan M., San S. E., Köysal O., (2005), "Dielectric spectroscopy analysis of molecular reorientation in dye doped nematic liquid crystals having different preliminary orientation", *Dyes and Pigments*, 65(2), 169-174.
- [37] Okutan M., Köysal O., San S. E., Köysal Y., (2012), "Electrical Parameters of Different Concentrations of Methyl Red in Fullerene Doped Liquid Crystal", *ISRN Nanomaterials*, 2012 1-5.
- [38] Yalcin O., Coskun R., Okutan M., Ozturk M., (2013), "Comparison effects and dielectric properties of different dose methylene-blue-doped hydrogels", *Journal of Physical Chemistry B*, 117(30), 8931-8938.

- [39] Yasin M., Tauqeer T., Karimov K. S., San S. E., Kösemen A., Yerli Y. Tunc A. V., (2014), "P3HT:PCBM blend based photo organic field effect transistor", *Microelectronic Engineering*, 130(2), 13-17.
- [40] Yang S. Y., Kim S. H., Shin K., Jeon H. Park C. E., (2006), "Low-voltage pentacene field-effect transistors with ultrathin polymer gate dielectrics", *Applied Physics Letters*, 88(17), 173507-173516.
- [41] Nakai I. F., Tachioka M., Ugawa A., Ueda T., Watanabe K. Matsumoto Y., (2009), "Molecular structure and carrier distributions at semiconductor/dielectric interfaces in organic field-effect transistors studied with sum frequency generation microscopy", *Applied Physics Letters*, 95(24), 243304-2043307,
- [42] Guo T.-F., Tsai Z.-J., Chen S.-Y., Wen T.-C. Chung C.-T., (2007), "Influence of polymer gate dielectrics on n-channel conduction of pentacene-based organic field-effect transistors", *Journal of Applied Physics*, 101(12), 124505-124511.
- [43] Tunç A. V., (2012), "Optimization of the performance of polymer based field effect transistors by tuning intrinsic properties and film nanomorphology", Doctor of Philosophy Thesis, Carl von Ossietzky Universität Oldenburg.
- [44] Kösemen A., San S. E., Okutan M., Doğruyol Z., Demir A., Yerli Y., Şengez B., Başaran E. Yılmaz F., (2011), "A novel field effect transistor with dielectric polymer gel", *Microelectronic Engineering*, 88(1), 17-20.
- [45] Vladimir Burtman A. Z., Andrei V. Pakoulev, (2011), "Molecular Photovoltaics in Nanoscale Dimension", *International Journal of Molecular Science*, 12, 173-225.
- [46] Wöll C., (2009) "Organic Electronics", 5, WILEY-VCH Verlag GmbH & Co. KGaA.
- [47] Don Park Y., Lim J. A., Lee H. S. Cho K., (2007), "Interface engineering in organic transistors", *Materials Today*, 10(3), 46-54.
- [48] Luca Valentini. Marta Cardinali M. M., Petar Uskokovic, Federico Alimenti, Luca Roselli, Josè Kenny, (2013), "Flexible transistors exploiting P3HT on paper substrates and graphene oxide films as gate dielectrics: proof of concept", *Science of Advanced Materials*, 5(5), 530-534.
- [49] S.W. Lina Y. M. S., A.M. Songa, (2010), "Enhanced stability of poly(3-hexylthiophene) transistors with optimally cured poly(methyl methacrylate) dielectric layers", *Synthetic Metals*, 160, 2430,2435.

BIOGRAPHY

Çiğdem Çakırlar was born in Diyarbakır, 1990. She had lived in Tuzla, İstanbul till 2008. She had started Engineering Physics (English) at University of Gaziantep in 2008. She has taken her bachelor degree in 2013 as second student on department with honor degree. Right after bachelor degree she has started to study in Physics Department as master student in Gebze Institute of Technology (GIT). She was awarded with National Scholarship for Graduate Student by TUBITAK. Still she is researcher on Organic Electronic Group of physics department, GTU.